Available online at www.sciencedirect.com

ScienceDirect

Nuclear Physics A

Nuclear Physics A 00 (2020) 1–4

www.elsevier.com/locate/procedia

XXVIIIth International Conference on Ultrarelativistic Nucleus-Nucleus Collisions
(Quark Matter 2019)

Dijet Acoplanarity in CUJET3 as a Probe of the Nonperturbative Color Structure of QCD Perfect Fluids

M. Gyulassy[a,b], P.M. Jacobs[a], J. Liao[c], S. Shi[d], X.N. Wang[a,b], F. Yuan[a]

[a] Nuclear Science Division, Lawrence Berkeley National Laboratory, Berkeley, CA 94720, USA
[b] Institute of Particle Physics, Central China Normal University, Wuhan, China
[c] Physics Department and Center for Exploration of Energy and Matter, Indiana University, 2401 N Milo B. Sampson Lane, Bloomington, IN 47408, USA
[d] Dept. of Physics, McGill University, 3600 rue University, Montreal, QC H3A 2T8, Canada

See also MG, QM18 talk, Nucl.Phys. A982 (2019) 627-630

MG@QM18

a+b=q+g approx

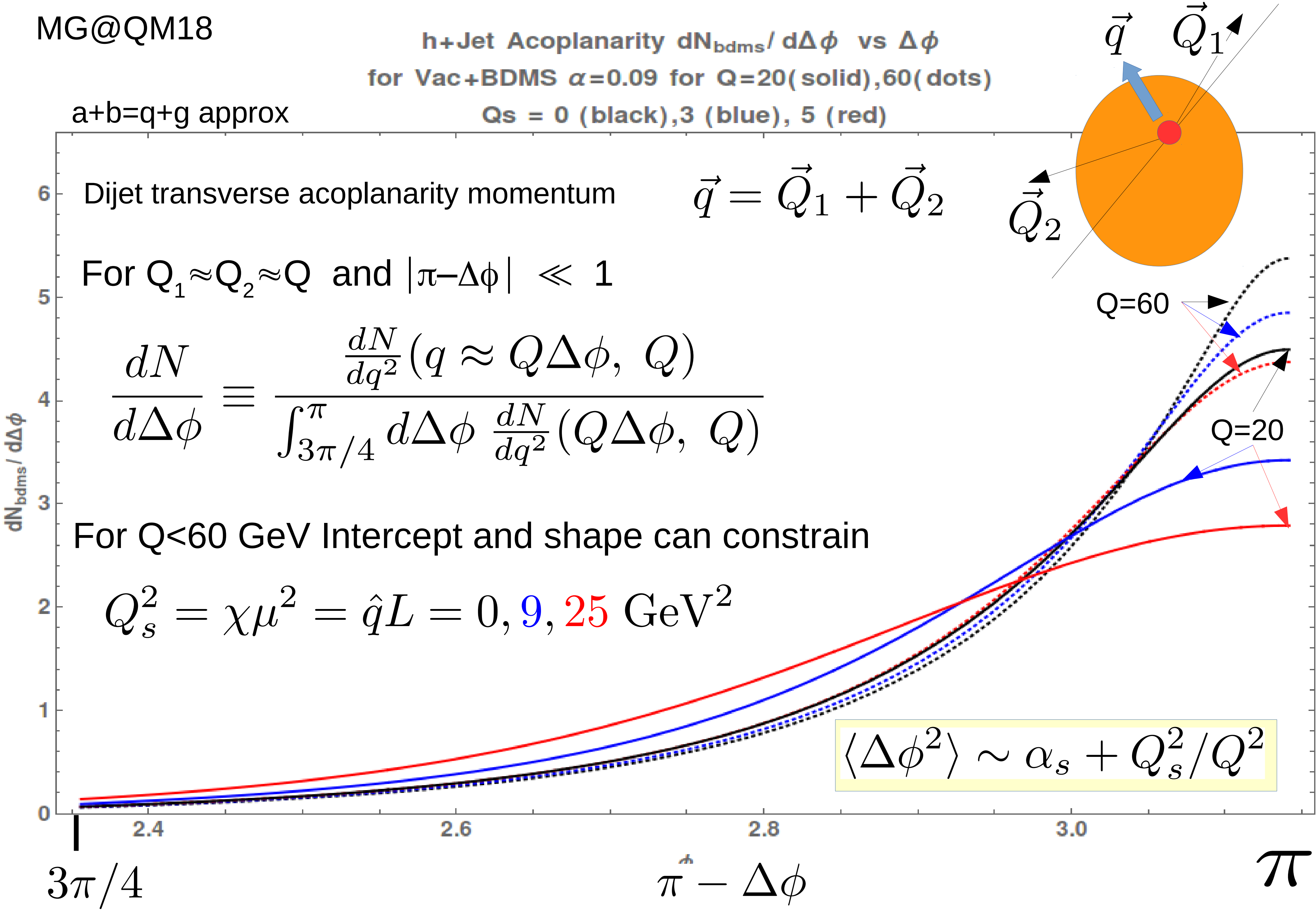

Dijet transverse acoplanarity momentum $\vec{q} = \vec{Q}_1 + \vec{Q}_2$

For $Q_1 \approx Q_2 \approx Q$ and $|\pi - \Delta\phi| \ll 1$

$$\frac{dN}{d\Delta\phi} \equiv \frac{\frac{dN}{dq^2}(q \approx Q\Delta\phi,\ Q)}{\int_{3\pi/4}^{\pi} d\Delta\phi\ \frac{dN}{dq^2}(Q\Delta\phi,\ Q)}$$

For Q<60 GeV Intercept and shape can constrain

$$Q_s^2 = \chi\mu^2 = \hat{q}L = 0, 9, 25\ \mathrm{GeV}^2$$

$$\langle \Delta\phi^2 \rangle \sim \alpha_s + Q_s^2/Q^2$$

M.Gyulassy et al, NPA 982 (2019) 627

What ***is*** QCD Fluid Matter ?? What are its effective degrees of freedom ??

Section 1: Motivation and Results

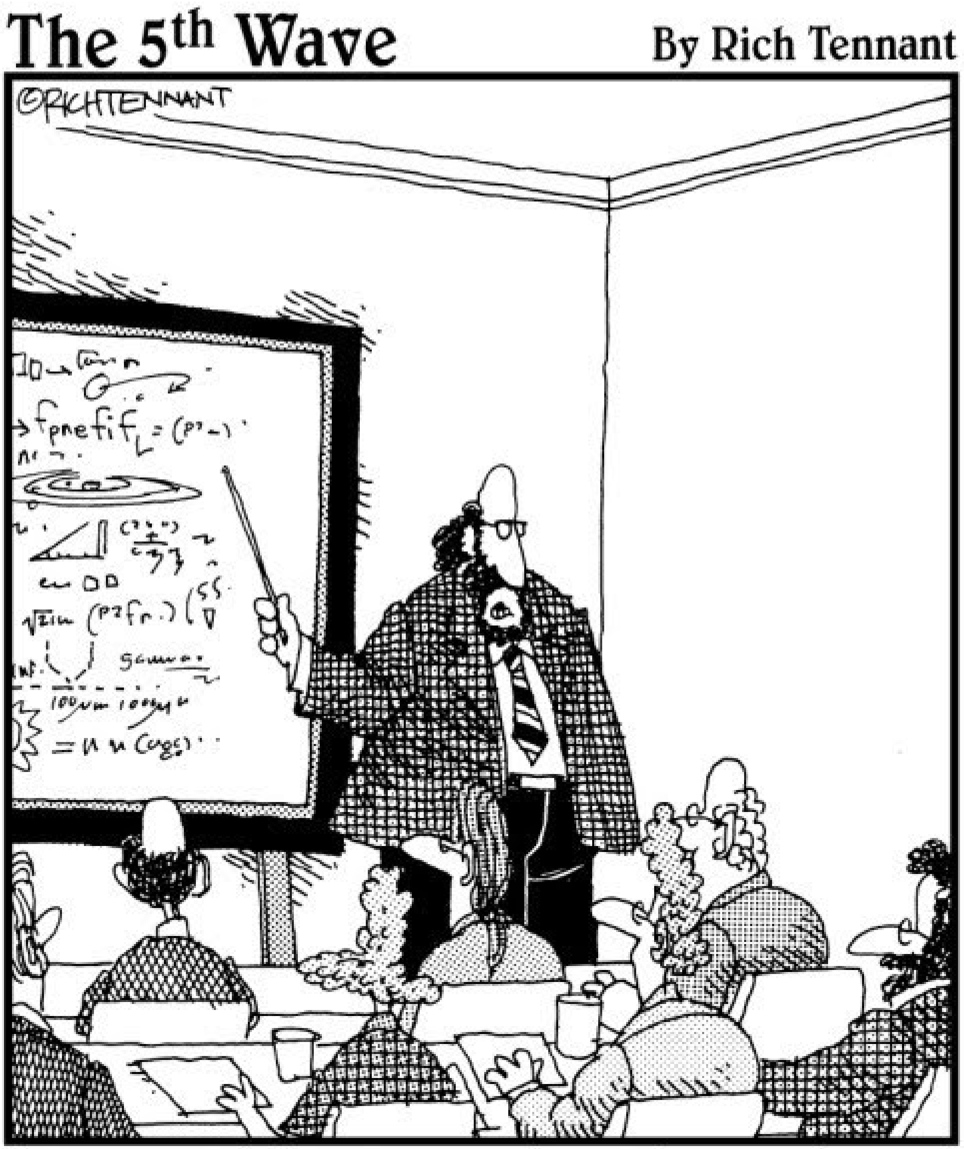

"Along with 'Antimatter,' and 'Dark Matter,' we've recently discovered the existence of 'Doesn't Matter,' which appears to have no effect on the universe whatsoever."

Can RAA & v2 Constrained Acoplanarity In A+A help Answer this?

Fortunately, CUJET3 can make falsifiable predictions with wQGP and sQGMP dof
That may help in the future to break degeneracies of current A+A data interpretations

Motivation: **J. Liao and E. Shuryak**, Angular Dependence of Jet Quenching Indicates Its Strong Enhancement Near the QCD Phase Transition ,**PRL(2009); Shuryak PRC66 (2002)**

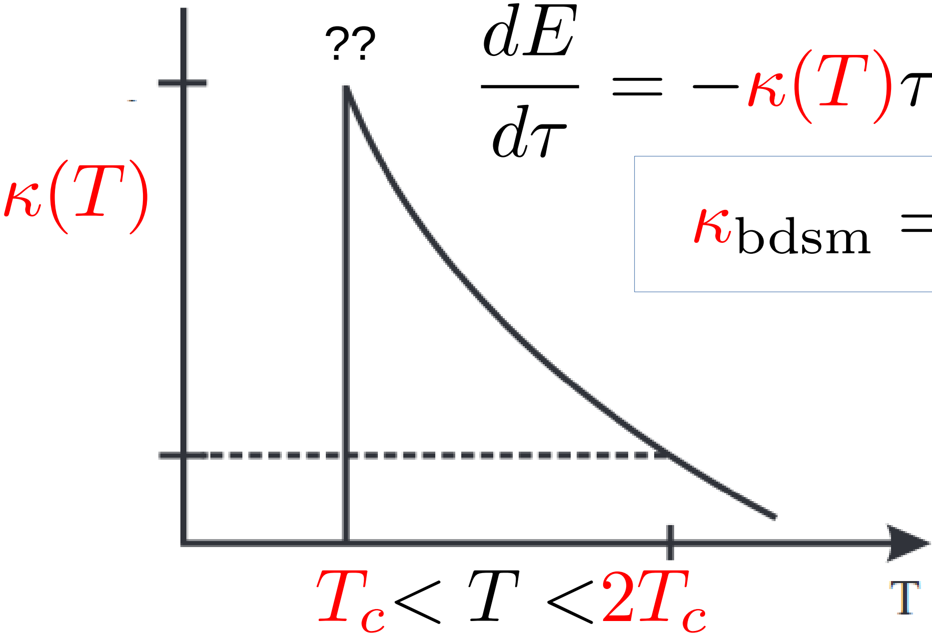

$$\frac{dE}{d\tau} = -\kappa(T)\tau^b T^{2+b}$$

$$\kappa_{\rm bdsm} = \hat{q}/T^3$$

$$\frac{d\Delta\phi^2}{d\tau} = +\kappa(T)\frac{T^3}{E^2}$$

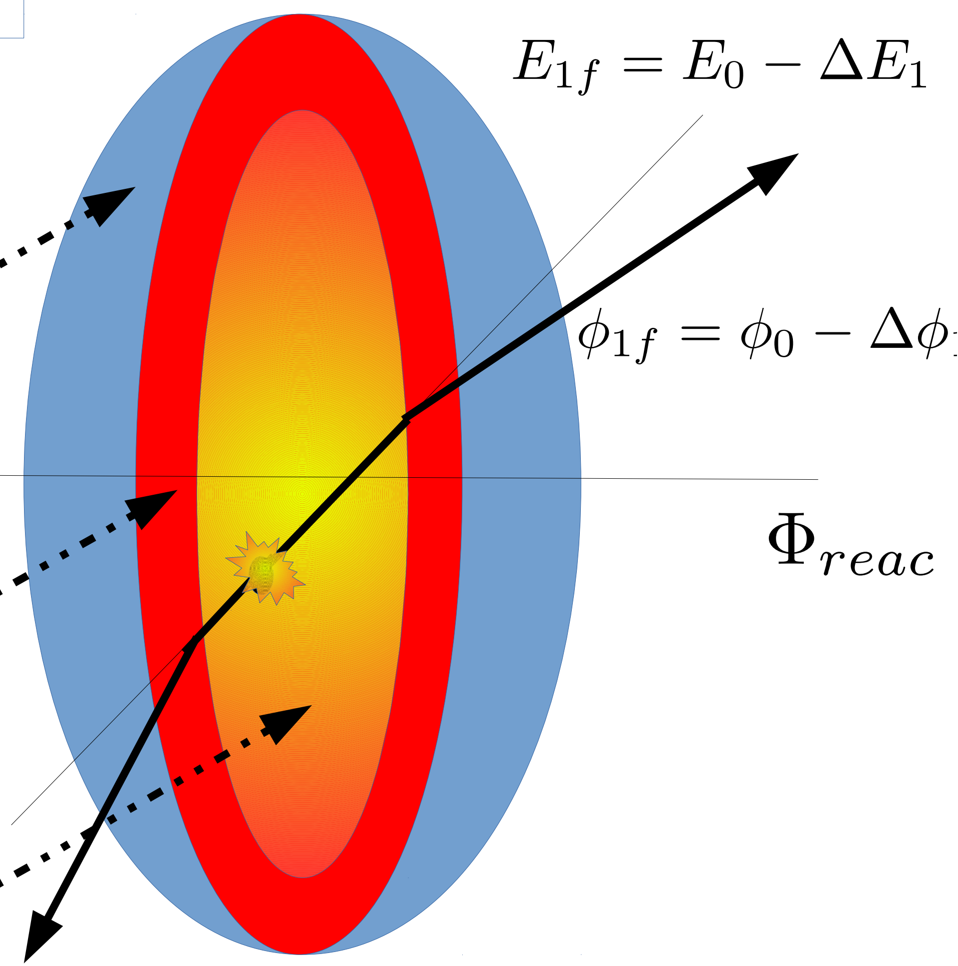

T < Tc

"Crossover Region"

T ~(1-2) Tc

T > 2 Tc

The main Idea:
Emergent
Color Magnetic
Monopole d.o.f
near Tc can enhance
jet ΔE and v_2 (*and* $\Delta\phi$)
due to jet- monopole
Dirac constraint:

$$\alpha_E \alpha_M \geq 1 \gg \alpha_E^2$$

$$E_{2f} = E_0 - \Delta E_2 \qquad \phi_{2f} = \pi + \phi_0 - \Delta\phi_2$$

=> a κ peak near (1-2) Tc should
Enhance jet azimuthal asymmetry
and dijet acoplanarity !

But how much??

Chinese Physics C Vol. 42, No. 10 (2018) 104104

Probing the color structure of the perfect QCD fluids via soft-hard-event-by-event azimuthal correlations*

施舒哲 廖劲峰 许乐世
Shuzhe Shi[1)] Jinfeng Liao[1;1)] Miklos Gyulassy[2,3,4]

$P/T = \rho_q + \rho_g + \rho_m$ vs $P/T = \rho_q + \rho_g$

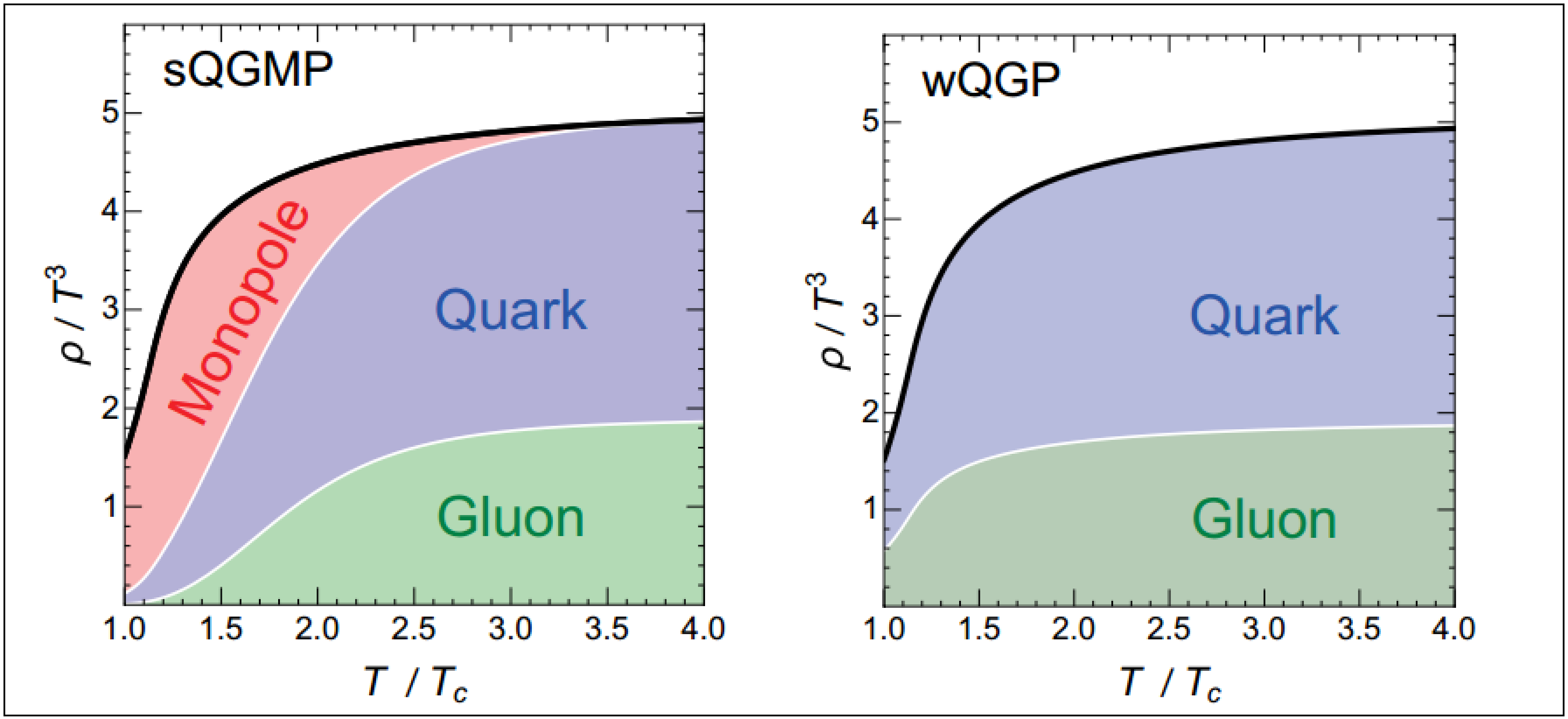

CUJET3 = (OSU VISHNU)(soft hydro) + DGLV(hard jets) + sQGMP

CIBJET = event-by-event CUJET3

Jiechen Xu et al
Shuzhe Shi et al

CUJET3 **sQGMP** composition constrained by **Lattice QCD** thermo P(T), L(T), $\chi^u(T)$, $\mu_E(T)$, $\mu_M(T)$

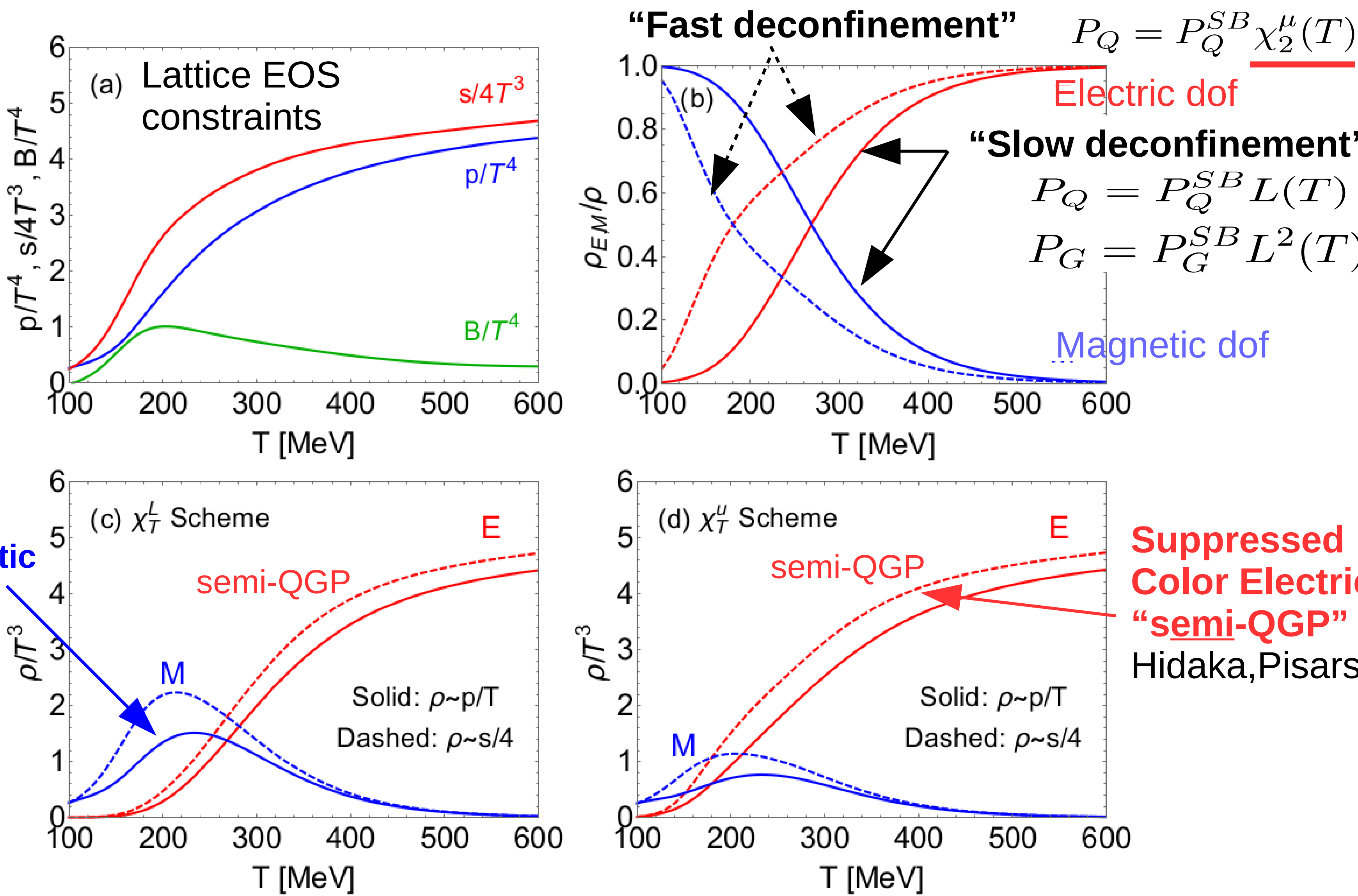

Emergent Color Magnetic Monopole d.o.f.
Shuryak, Liao

Suppressed Color Electric "semi-QGP"
Hidaka,Pisarski

sQGMP is a lattice QCD constrained phenom realization of **t'Hooft, Polyakov and Mandelstam 1974** proposal that emergent color Magnetic Monopole d.o.f. may play a dominant role confining the color electric q and g d.o.f. below T < Tc ~ 160 MeV via a magnetic dual of Meissner effect

(See also B.Zakharov:1412.6287; Ramamurti, Shuryak, Zahed, 1802.10509)

Radiative energy loss in CUJET= DGLV generalized to sQGMP

$$\Gamma_a = \sum_b \rho_b(T)\, d^2\sigma_{ab}(T)/d^2 q_\perp$$

$$\begin{aligned}
\frac{\Delta E_{\rm rad}}{E} &= \int x_E \frac{dN}{dx_E} dx_E \\
&= \frac{18 C_R}{\pi^2}\frac{4+N_f}{16+9N_f}\int d\tau\; \rho(\mathbf{z})\Gamma(\mathbf{z}) \int d^2\mathbf{q}_\perp \frac{1}{\mathbf{q}_\perp^2}\left[\frac{\alpha_s^2\chi_T f_E^2}{\mathbf{q}_\perp^2+f_E^2\mu^2(\mathbf{z})}+\frac{(1-\chi_T)f_M^2}{\mathbf{q}_\perp^2+f_M^2\mu^2(\mathbf{z})}\right] \\
&\times \int_0^1 dx_+ \int d^2\mathbf{k}_\perp \alpha_s\Big(\frac{\mathbf{k}_\perp^2}{x_+(1-x_+)}\Big)\left[1-\cos\left(\frac{(\mathbf{k}_\perp-\mathbf{q}_\perp)^2+\chi^2(\mathbf{z})}{2x_+E}\tau\right)\right]\left(1+\frac{\mathbf{k}_\perp^2}{4x_+^2E^2}\right) \\
&\times \frac{-2(\mathbf{k}_\perp-\mathbf{q}_\perp)}{(\mathbf{k}_\perp-\mathbf{q}_\perp)^2+\chi^2(\mathbf{z})}\left[\frac{\mathbf{k}_\perp}{\mathbf{k}_\perp^2+\chi^2(\mathbf{z})}-\frac{(\mathbf{k}_\perp-\mathbf{q}_\perp)}{(\mathbf{k}_\perp-\mathbf{q}_\perp)^2+\chi^2(\mathbf{z})}\right]
\end{aligned}$$

N=0 & 1 Interference
"Antenna"

In order to derive the HT qhat approximation from above we must expand the 2nd *and* 3rd lines in powers of $\mathbf{q}_\perp$ **and retain only the quadratic $\mathbf{q}_\perp^2$ term !! But all higher moments DIVERGE!**
in E→ ∞ limit

$$\begin{aligned}
&\approx \frac{24}{\pi^2}\frac{4+N_f}{16+9N_f}\int d\tau \left\{\hat{q}(\tau) = \int d^2q_\perp\, q_\perp^{\mathbf{2}}\,\Gamma_a(\tau,\mathbf{q}_\perp) = dQ_s^2(\tau)/d\tau\right\} \\
&\times \left\{\int_0^1 dx_+ \int d^2\mathbf{k}_\perp \alpha_s\Big(\frac{\mathbf{k}_\perp^2}{x_+(1-x_+)}\Big)\left[1-\cos\left(\frac{\mathbf{k}_\perp^2+\chi^2(\mathbf{z})}{2x_+E}\tau\right)\right]\left(1+\frac{\mathbf{k}_\perp^2}{4x_+^2E^2}\right)\frac{2(\mathbf{k}_\perp^2-\chi^2(\mathbf{z}))^2}{(\mathbf{k}_\perp^2+\chi^2(\mathbf{z}))^4}\right. \\
&\left. + \int_0^1 dx_+ \int d^2\mathbf{k}_\perp \alpha_s\Big(\frac{\mathbf{k}_\perp^2}{x_+(1-x_+)}\Big)\left[\sin\left(\frac{\mathbf{k}_\perp^2+\chi^2(\mathbf{z})}{2x_+E}\tau\right)\frac{\mathbf{k}_\perp^2\tau}{x_+E}\right]\left(1+\frac{\mathbf{k}_\perp^2}{4x_+^2E^2}\right)\frac{\mathbf{k}_\perp^2-\chi^2(\mathbf{z})}{(\mathbf{k}_\perp^2+\chi^2(\mathbf{z}))^3}\right\}
\end{aligned}$$

We found that the int dx integral of 2nd *and* 3rd lines of this asymptotic series behave approximately linearly in path time only in the formal E→ ∞ limit ! But For E<100 GeV and T<400 MeV CUJET energy loss does not reduce to BDMS form

$$\Delta E_s(CUJET) \neq \Delta E_s(BDMS) \propto \int dt\, t^1\, \hat{q}_a(x(t),t)$$

$$F(\Omega t, \Omega/E) = \int_{\Omega/E}^{1} dx\{1 - Cos[\Omega^2 t/(2xE)]\} \propto (\Omega t)^{\gamma(\Omega t, \Omega/E)}$$

Formation time index

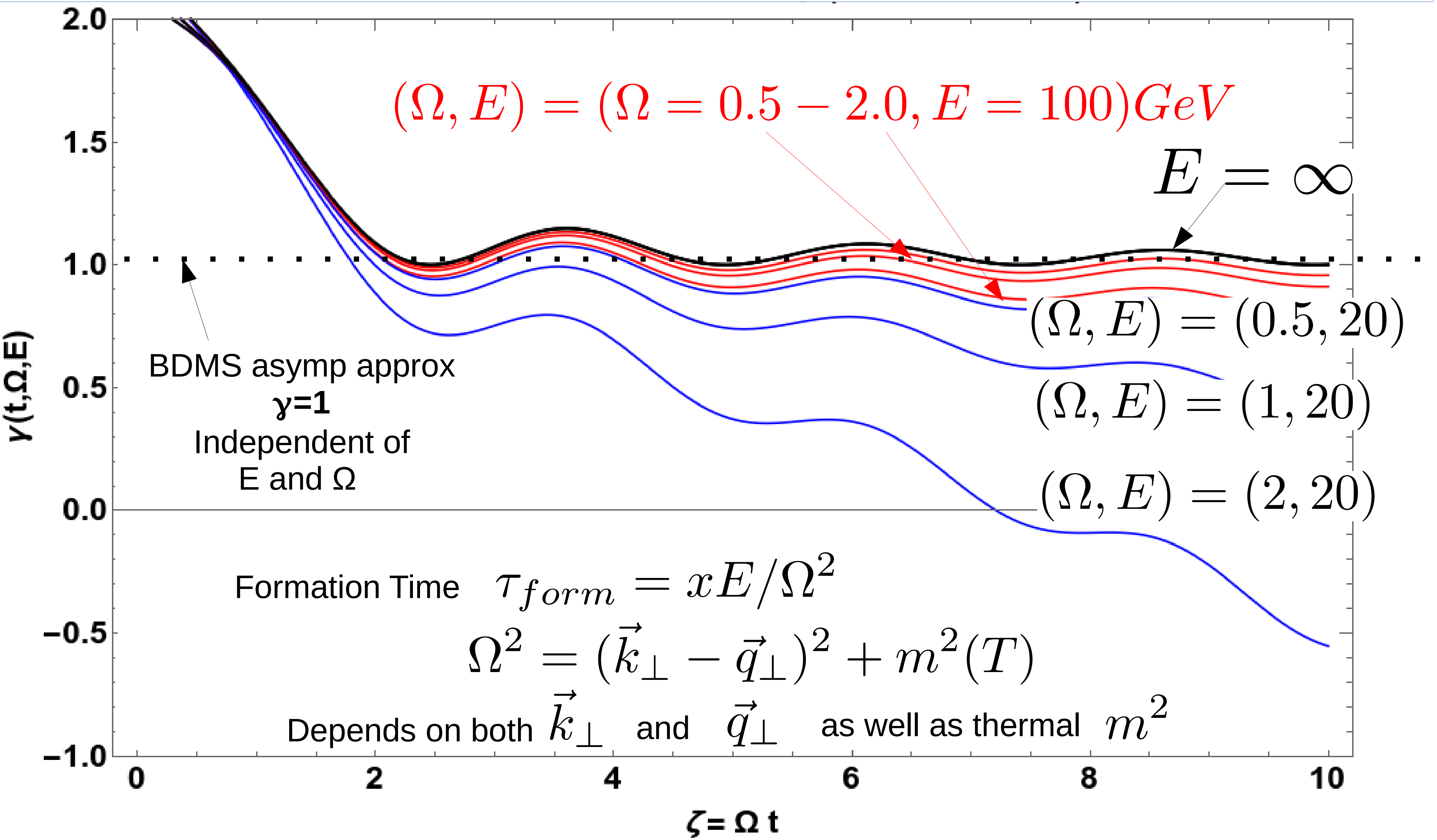

CUJET3: T and E dependence of Jet transport coef $\hat{q}(T,E)$ constrained by RHIC&LHC R_{AA}

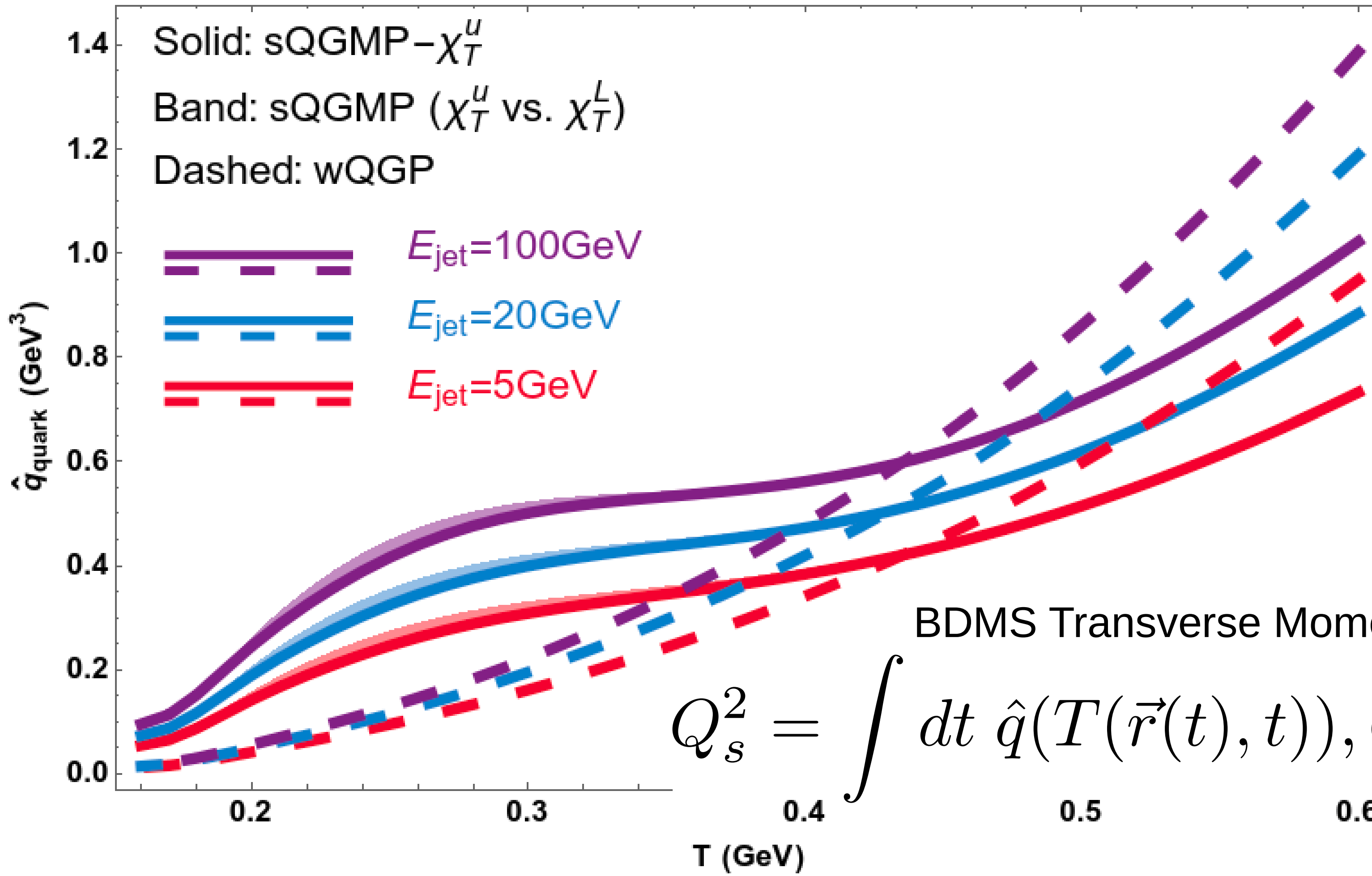

BDMS Transverse Momentum Scale

$$Q_s^2 = \int dt\ \hat{q}(T(\vec{r}(t),t)),Q) = \langle \hat{q} L \rangle$$

E+E dof

E+M dof

$$\hat{q}_F(E,T) = \int_0^{6ET} dq_\perp^2 \frac{2\pi}{(\boldsymbol{q}_\perp^2 + f_E^2\mu^2(\boldsymbol{z}))(\boldsymbol{q}_\perp^2 + f_M^2\mu^2(\boldsymbol{z}))}\rho(T)$$
$$\times \Big\{ [C_{qq}f_q + C_{qg}f_g] \cdot \boxed{[\alpha_s^2(\boldsymbol{q}_\perp^2)]} \cdot [f_E^2\boldsymbol{q}_\perp^2 + f_E^2 f_M^2\mu^2(\boldsymbol{z})] +$$
$$[C_{qm}(1-f_q-f_g)] \cdot \boxed{[1]} \cdot [f_M^2\boldsymbol{q}_\perp^2 + f_E^2 f_M^2\mu^2(\boldsymbol{z})] \Big\},$$

Summary 1: CUJET3= VISHNU+DGLV global RAA constrained jet transport fields

$\hat{q}(T,E)$ VISHNU $T(x,0,t)$ $\hat{q}(T(x,0,t),E)$

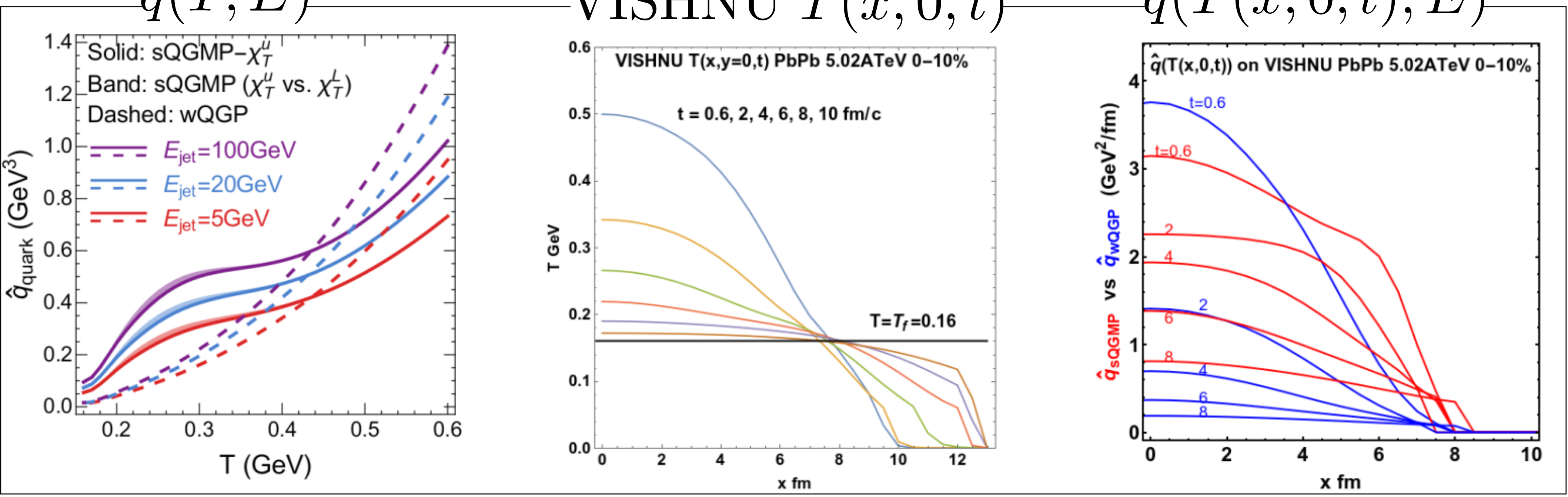

Fig. 1. (color online) (Left) The CUJET3.1 R_{AA} constrained [16, 17, 18, 19] jet transport field, $\hat{q}_F(T,E)$ for quark jets with E_{ini} = 5, 20, 100 GeV are compare to wQGP and sQGMP models of the chromo electric and magnetic dof in the QCD fluid. Dashed curves for wQGP assume only color di-electric dof while solid curves for sQGMP assume that the color electric quark and gluon dof are suppressed by lattice Polyakov, $L(t)$, or susceptibility, χ_T^u, due to partial confinement 160 $<T<$ 320 MeV range and assume that emergent that the remaining dof are color magnetic monopole dof that condense across the QCD crossover temperature range. (Center) Isochronous evolution of temperature field, $T(x,0,t)$, in VISHNU2+1 viscous hydrodynamics[13] for 0-10% $Pb+Pb$ 5.02ATeV. (right) The isochronous evolution of the jet transport coefficient, $\hat{q}(T(x,0,t),E=20$ GeV), for a quark jet of energy 20 GeV in the VISHNU temperature field shown in the middle panel. Blue isochrones show $\hat{q}_{wQGP}$. Red isochrones show $\hat{q}_{sQGMP}$, Note that $\hat{q}_{sQGMP}$ is strongly enhanced in the surface regions and at late times close to freeze-out.

Summary 2: CUJET3 PbPb 5.02ATeV Partonic Level RAA and v2 jet-medium observables

partonic R_{AA} are same in sQGMP and wQGP
Because dynamical $\{\alpha(T_c),\ \mu_M/\mu_E\}$ params are fixed by ***global*** RHIC & LHC χ^2 fits to charged hadron $R_{AA}(p_T>20, s=0.2\text{-}5\ \mathrm{TeV}, \%)$

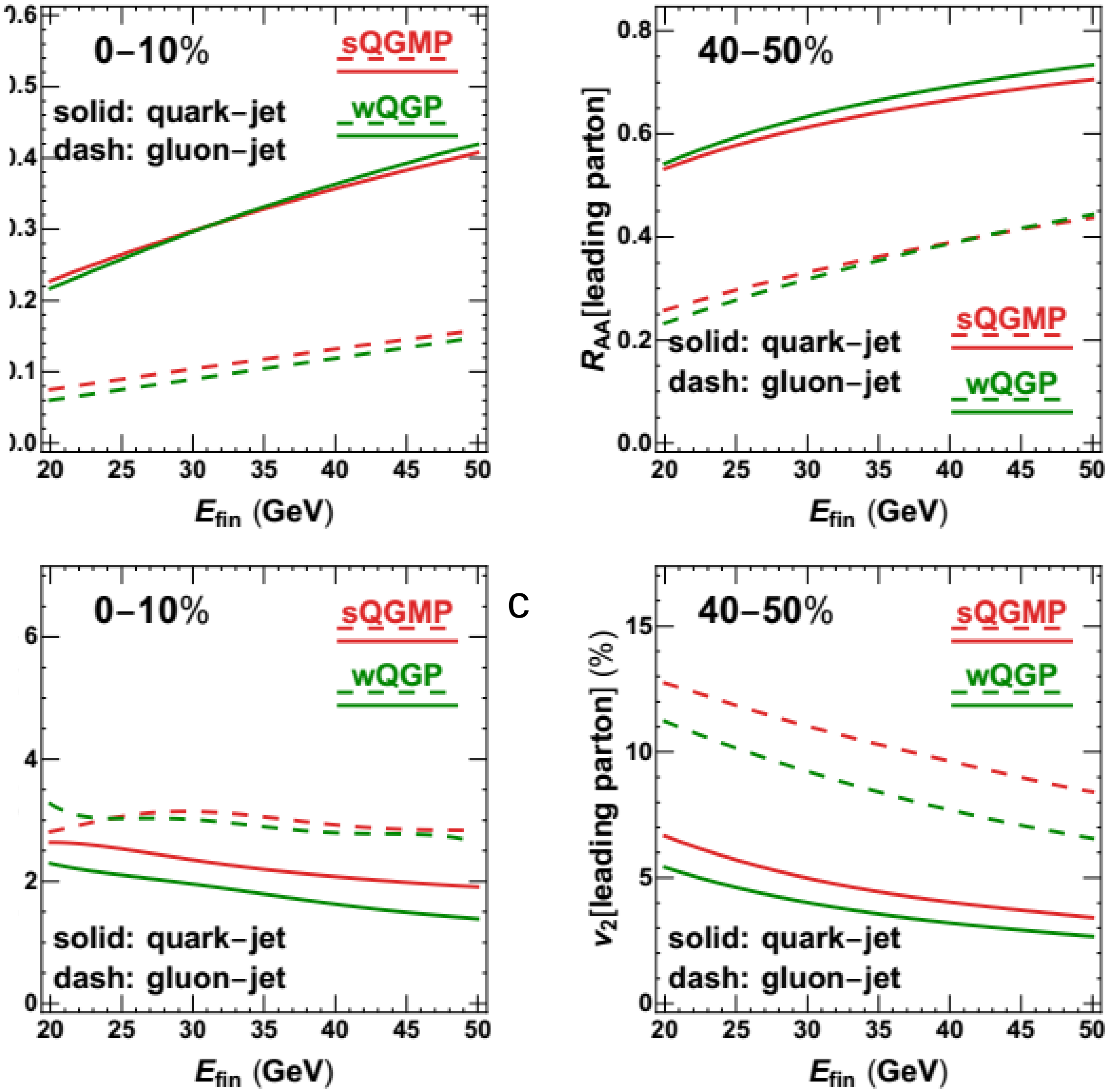

Partonic v2 differ in sQGMP and wQGP because Magnetic Monopoles in sQGMP enhance qhat in high eccentricity surface regions

Tc < T(x,t) < 2Tc

FIG. 4. Angular average (R_{AA}) and azimuthal anisotropy (v_2) of modification factor $R_{AA}(\hat{\boldsymbol{n}}; E_{\rm fin})$ for leading light quarks (solid) and gluons (dash) with different final energy $E_{\rm fin}$, with different schemes of color constituent (different colors). Left and right panels show results for 0–10%, and 40–50% centrality classes, respectively.

施舒哲 廖劲峰 许乐世 Chinese Physics C Vol. 42, No. 10 (2018) 104104

CIBJET (sQGMP) provides a $\chi^2/dof < 2$ solution to all RAA, v2, v3 data at RHIC and LHC

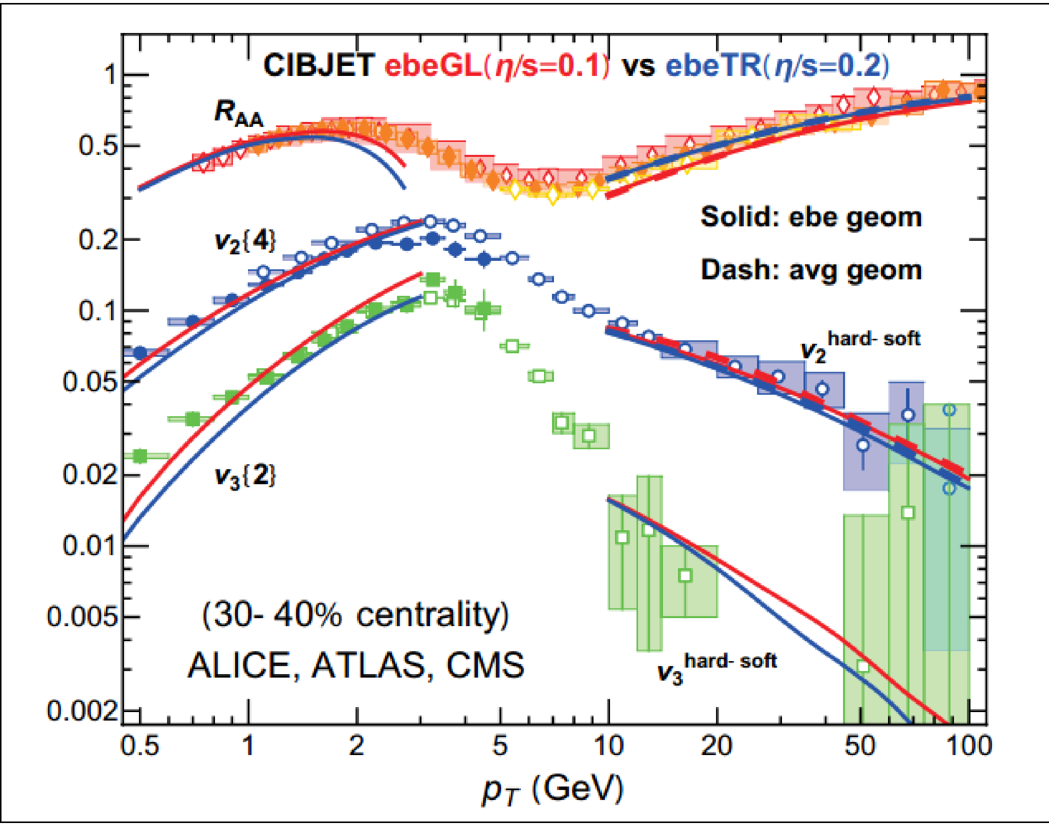

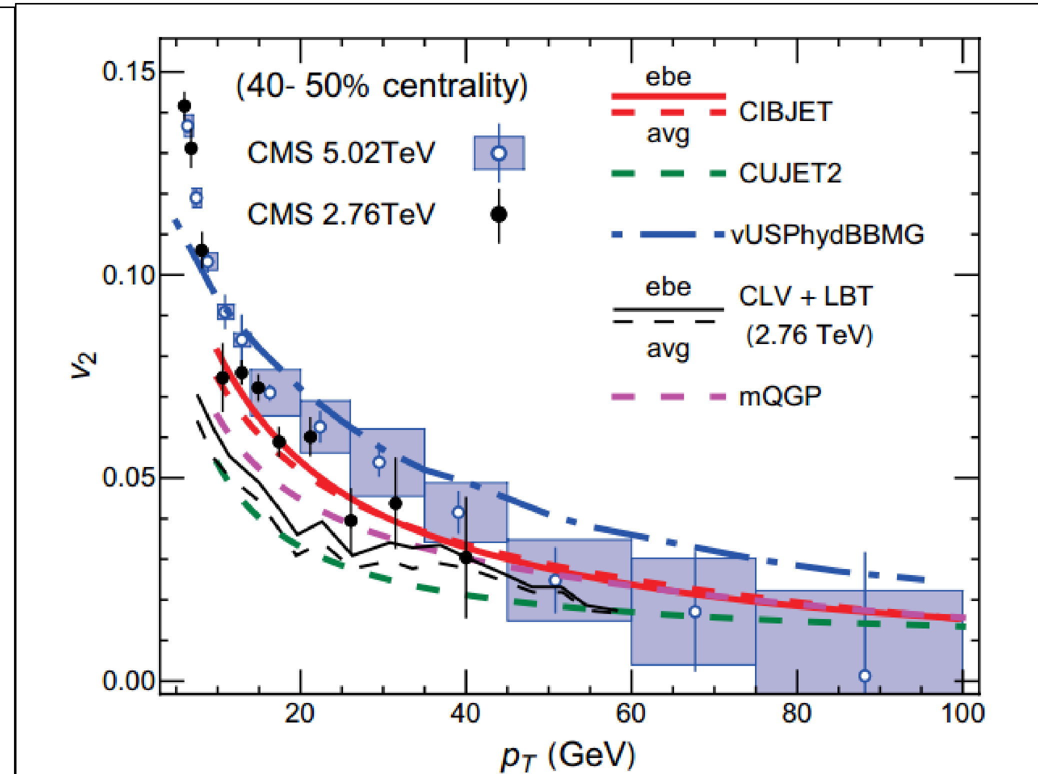

However other globally consistent RHIC+LHC RAA&v2 solutions also exist:

1. J. Noronha Hostler et al, PRL116,252301 (2016)
   “Event-by-Event Hydro +Jet Energy Loss: A Solution to the RAA⊗v2 Puzzle”

2. C. Andres et al, PoS HardProbes2018 (2019) 070
   “Constraining energy loss from high-T azimuthal asymmetries”

We need other observables to break theoretical degeneracies !
***Constrained* Dijet AcoplanarityTomography can help**

Acoplanarity distribution is a convolution of Vacuum Sudakov and Medium induced transverse deflection distributions (proposed as a QGP signal 34 years ago!)

D. A. Appel, PhysRD33, 717 (1986); J. P. Blaizot,L. D. McLerran, PRD34, 2739 (1986)
F.~D'Eramo et al, JHEP 1305 (2013) 031; 1901 (2019) 17; MG et al , QM18 NPA982 (2019) 627.

We utilize the acoplanarity formalism of

Mueller,Wu,Xiao,Yuan, PLB763, 208 (2016); PRD 95, 034007 (2017)
Chen,Qin,Wei,Xiao,Zhang, PLB773, 672 (2017)

$$\boxed{\frac{dN}{dq^2} \approx \frac{1}{Q^2}\frac{dN}{d\Delta\phi} = \int bdbJ_0(|q(Q,\Delta\phi)|b)e^{-S_{vac}(Q,b)-S_{med}(Q,b)}}$$

$$\boxed{S_{vac} \approx (\alpha/2\pi)\sum_{q,g}\left\{(A_1(\log(Q^2/\mu_b^2)^2/2 + (B_1 + D_1\log(1/R^2))\log(Q^2/\mu_b^2)\right\} + S_{NP}(Q,b)}$$

The medium induced broadening in **one parameter** multi soft **Gaussian** BDMS approximation

$$S_{BDMS}(b;Q_s) = b^2 Q_s^2/4 \qquad \boxed{Q_s^2 = \int dt\ \hat{q}(T(\vec{r}(t),t)),Q)}$$

The **two parameter** (opacity **χ=L/λ** and screening **μ**) GLV multiple Yukawa scatt approx:

$$S_{GLV}(b;\chi,\mu) = \chi(\mu b K_1(\mu b) - 1) \approx b^2\log[1/(b\mu)^2](\chi\mu^2)/4$$

Hadron-Jet acoplanarity azimuthal distribution from Chen,Qin,Xiao,Zhang PLB773, 2017
A+A Vacuum Sudakov+ BDMS(Q_s^2) and current RHIC and LHC data

Current State of "Acoplanarity Art"

L. Chen et al. / Physics Letters B 773 (2017) 672–676

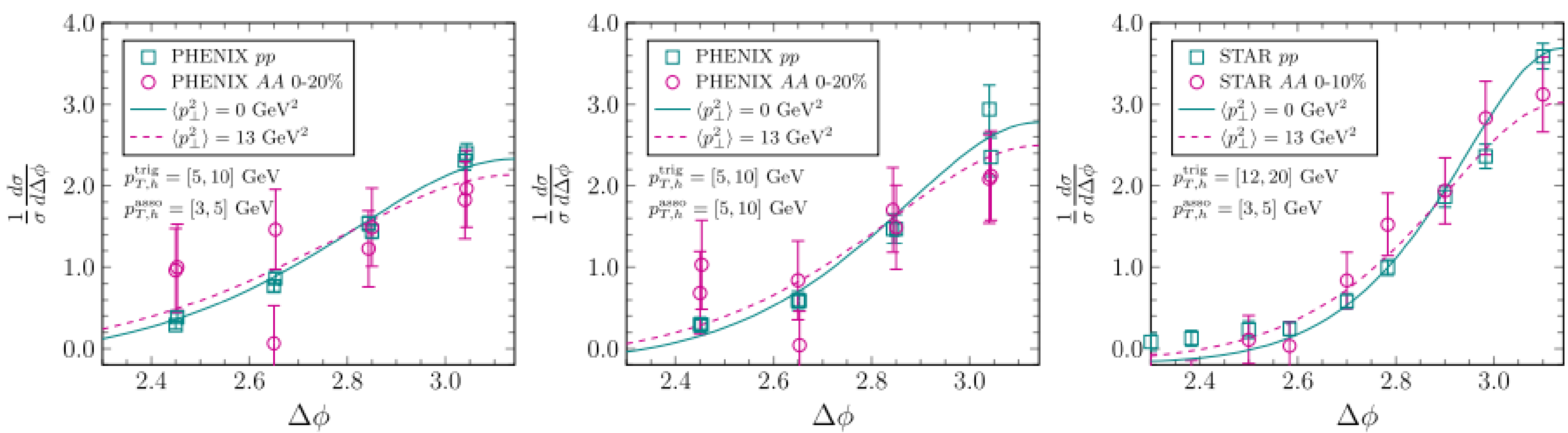

Fig. 1. Normalized dihadron angular correlation compared with PHENIX [51] and STAR [52] data.

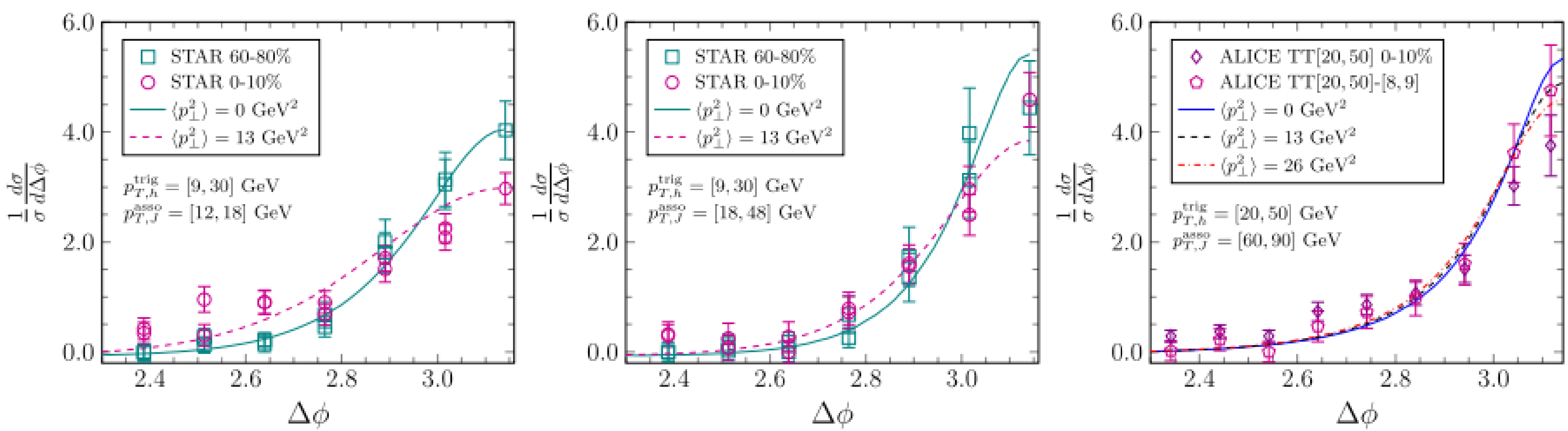

As a stand alone observable, Acoplanarity ***does not constrain*** Q_s^2 better than RAA&v2.
However, when constrained simultaneously with RAA&v2, Dijet Acoplanarity can greatly increases the exp discriminating power to the chromo structure of QCD fluids

CUJET3.1 Results for Single leading parton trigger

施舒哲 廖劲峰 许乐世

Constrained by global $\chi^2[\alpha_c, c_m;\ R_{AA}\ \&\ v_2]/d.o.f. < 2$

R_{AA} Constrained Parton Energy Loss

$$\langle \Delta \mathbf{E} \rangle_{sQGMP} \approx \langle \Delta \mathbf{E} \rangle_{wQGP}$$

CUJET3 Predicts factor ~2 enhancement of saturation scale in **sQGMP** vs **wQGP**

$$\langle \mathbf{Q_s^2} \rangle_{\mathbf{sQGMP}} \approx \mathbf{2} \times \langle \mathbf{Q_s^2} \rangle_{\mathbf{wQGP}}$$

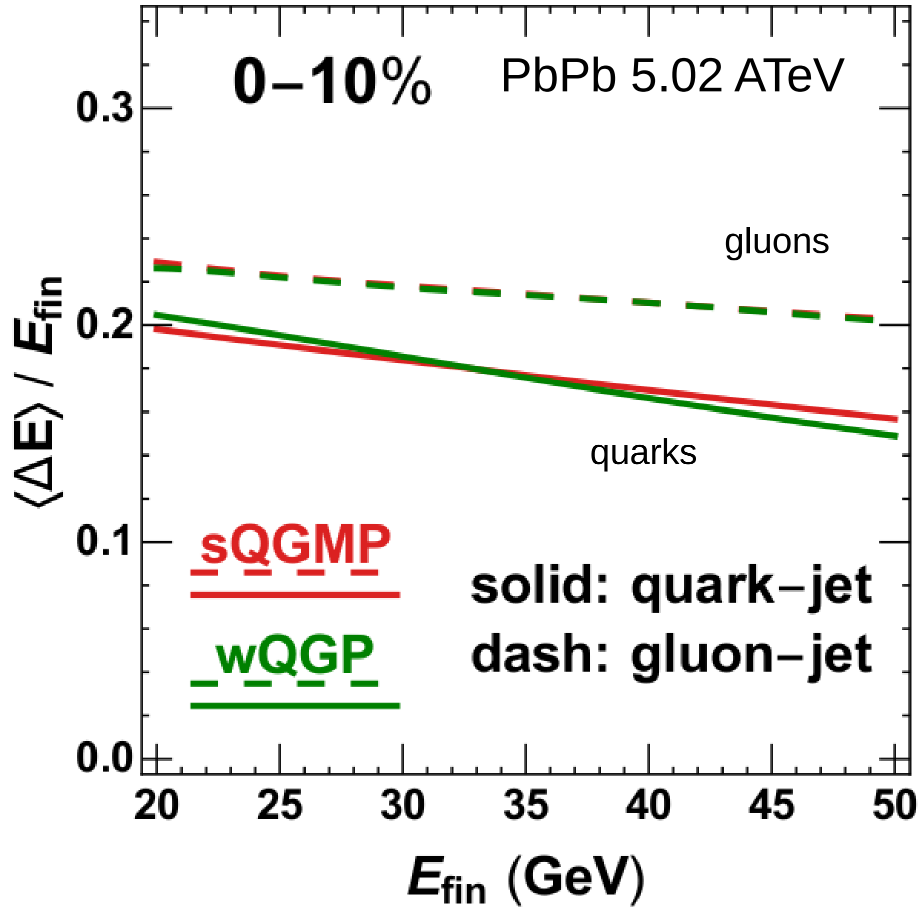

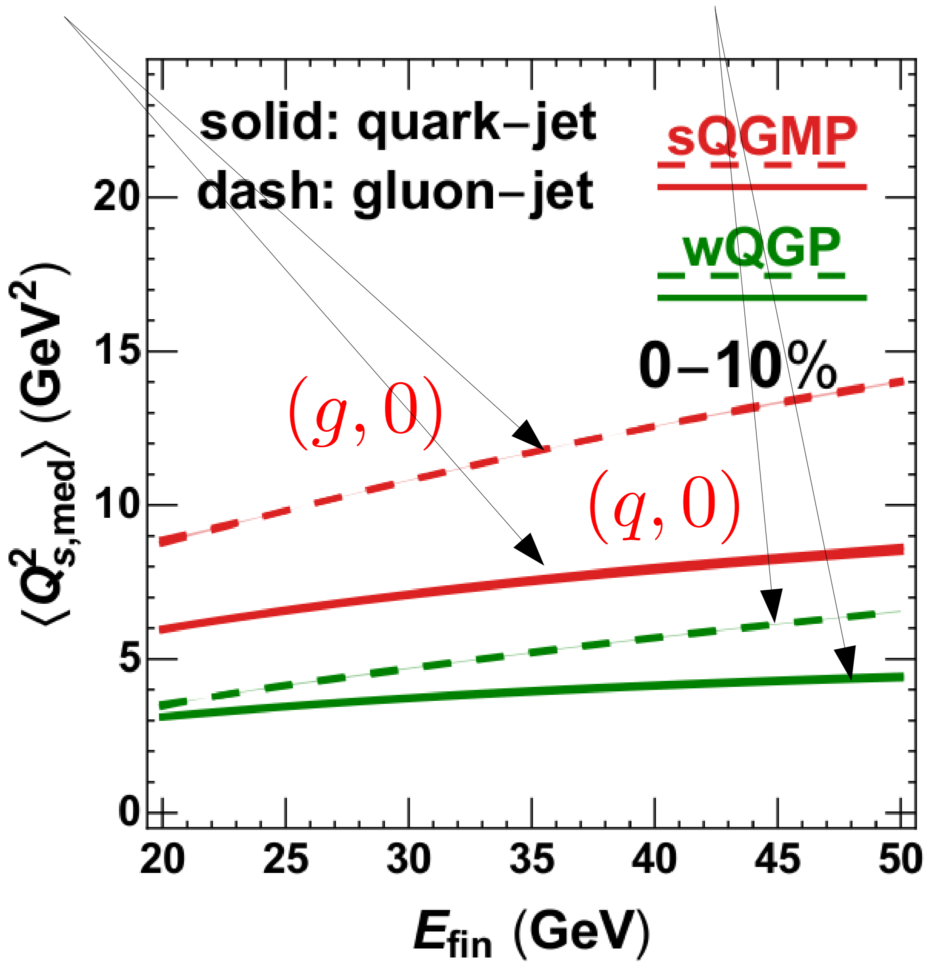

Summary 3: CUJET3= VISHNU+DGLV global RAA constrained **Dijet Acoplanarity**

$$Q_s^2 = \langle \hat{q} L \rangle \qquad \Delta\phi^2 = \langle Q_s^2 \rangle / E_{jet}^2 \qquad dN_{\rm dijet}/\Delta\phi$$

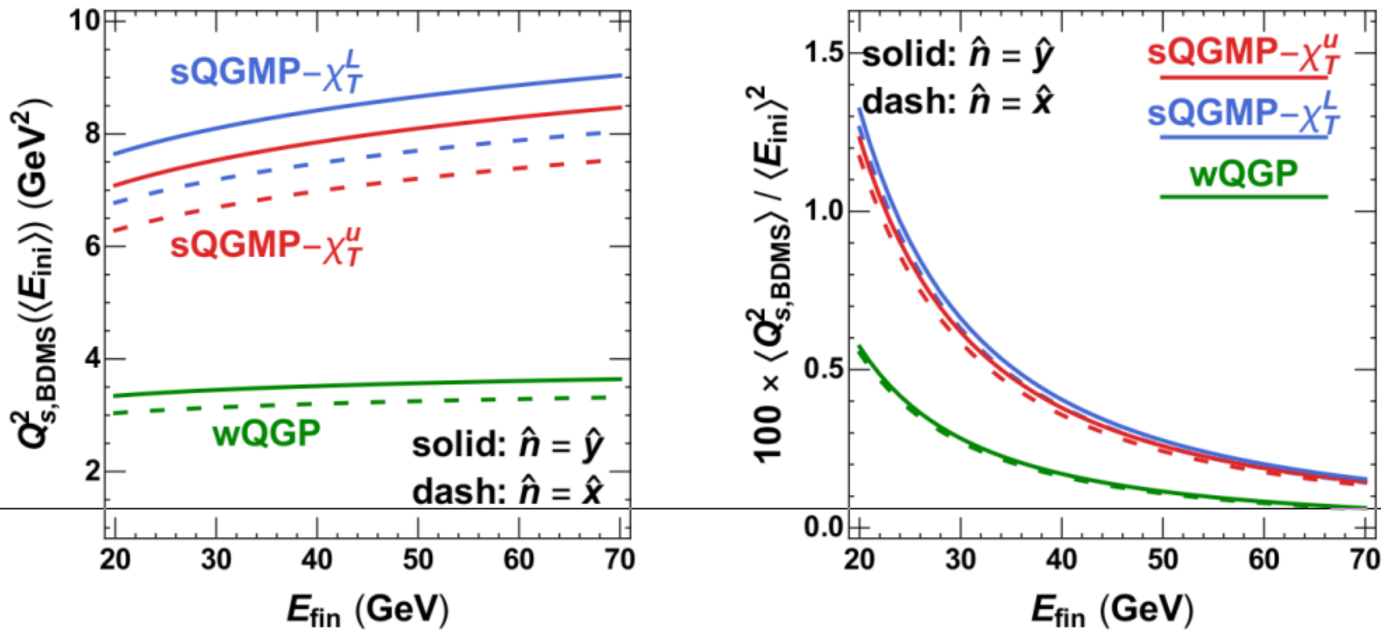

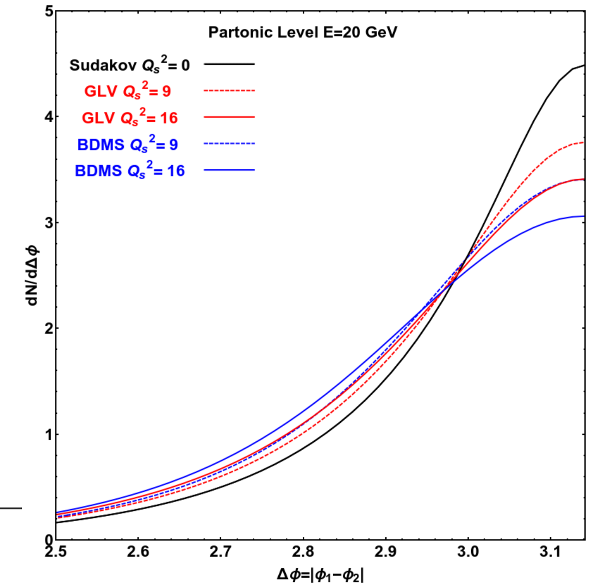

Semi-central 20-30% PbPb 5 ATeV qunched q and g jet spectra averaged case illustrated

Fig. 2. (Left) Comparison of CUJET3 path and q and g quenched jet spectra averaged parton level $Q_s^2[wQGP]$ (green) and $Q_s^2[sQGMP]$ (red and blue) as function of final quenched jet energy E_{fin} in central 20-30% Pb+Pb 5.02 ATeV using the $\hat{q}$ in Fig.1a. Solid curves compare results for initial jet moving in the $\hat{y}$ direction, out of plane while Dashed curves are for jets moving in plane. Only a very slight elliptic asymmetry of Q_s^2 is predicted. Green curves correspond to $Q_s^2(wQGP)$ vs E_{fin} without magnetic monopole dof. Red (Blue) curves correspond to $Q_s^2(sQGMP)$ with magnetic monopole dof in two schemes χ_T^u (χ_T^L), see [16]. Comparing red and blue curves to the green wQGP curves shows that emergent magnetic monopole dof in both sQGMP schemes approximately doubles the predicted Q_s^2 relative to the wQGP model without monopoles, even though both composition models are tuned to fit the same global R_{PbPb} data.

Percent level precision on $dN_{\rm dijet}/\Delta\phi$ to resolve magnetic monopole dof in QCD fluids,

Even though $\langle \mathbf{Q_s^2} \rangle_{\mathbf{sQGMP}} \approx \mathbf{2} \times \langle \mathbf{Q_s^2} \rangle_{\mathbf{wQGP}}$!!

CUJET3 Single parton “a” triggered **Dijet “a+b”** Summed Transverse Saturation Scales

$$\langle Q_s^2[ab](E_{fin} = E_{ini} - \Delta E^{a}(\mathbf{x}_0, \hat{\mathbf{n}})\rangle_{\{E_{ini}, \mathbf{x}_0, \hat{\mathbf{n}}\}}$$

Quenching probability

$$\langle Q^2_{s,\mathrm{med}}[a+b](\hat{\boldsymbol{n}}, E_{\mathrm{ini}})\rangle \equiv \int \mathrm{d}x_0 \mathrm{d}y_0 \int_{E_{\mathrm{fin}}}^{\infty} \mathrm{d}E_{\mathrm{ini}}\, P_a(\hat{\boldsymbol{n}}; x_0, y_0; E_{\mathrm{fin}} \leftarrow E_{\mathrm{ini}})\, \rho(\hat{\boldsymbol{n}}; E_{\mathrm{fin}}; x_0, y_0) \times \left[Q^2_{s,\mathrm{med}}[a](\hat{\boldsymbol{n}}, E_{\mathrm{ini}}; x_0, y_0) + Q^2_{s,\mathrm{med}}[b](-\hat{\boldsymbol{n}}, E_{\mathrm{ini}}; x_0, y_0)\right].$$

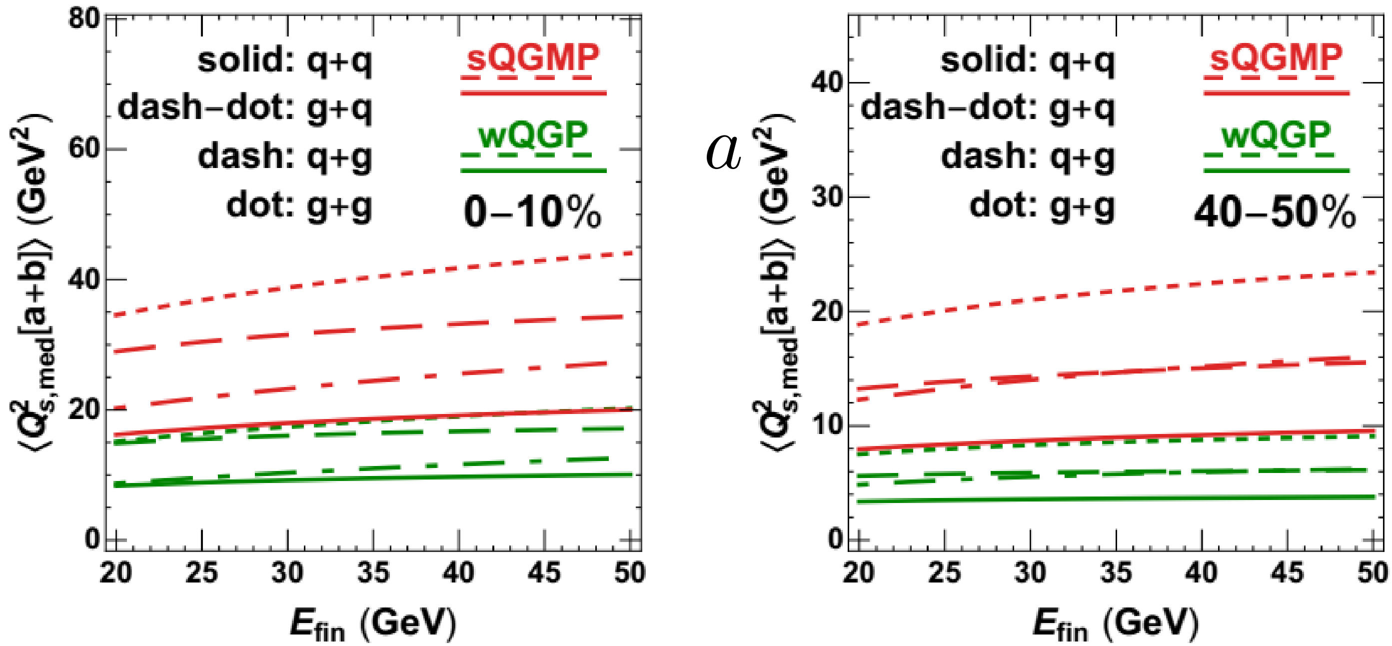

FIG. 7. Direction averaged di-jet medium saturation factor $Q^2_{s,\mathrm{med}}[a+b]$ with **single trigger** leading parton $[a]$ with final energy E_{fin}, assuming different schemes of color constituent (different colors). Triggering parton in [q+g] process is a light quark, while for [g+q] process is a gluon.

$$\langle \mathbf{Q}_s^2[ab]\rangle_{sQGMP} \approx 2 \times \langle \mathbf{Q}\rangle_s^2[ab]\rangle_{wQGP}$$

Enhancement approx Independent of dijet {a,b} channels

$$\frac{Q_s^2[a+b](sQGMP)}{Q_s^2[a+b](wQGP)} \sim 2$$

Also weak Dependence on trigger Efin

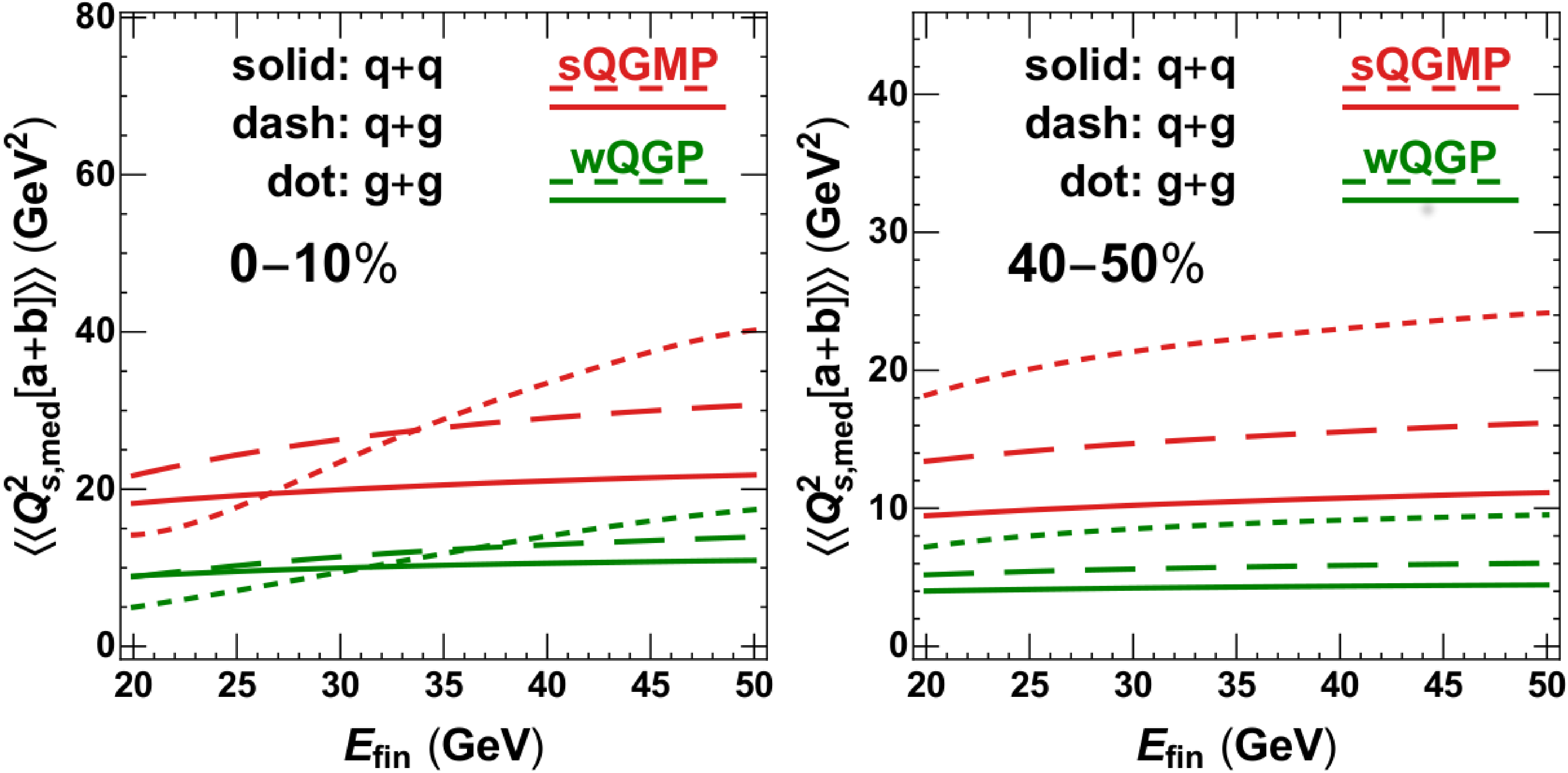

With dynamical parameters and hence quenched dijet *geometry* *Constrained* by RAA&v2 data, CUJET3 predicts that DiJet Acoplanarity dN/dϕ can discriminate Vacuum vs wQGP vs sQGMP color d.o.f. of the QCD fluid in the crossover T~ 150-300 MeV range for 20 < E < 60 GeV triggers in future 10 % precision level measurements in the BDMS (Gaussian) dipole approx:

$$S_{BDMS}(b;Q_s) = |b^2 Q_s^2/4$$

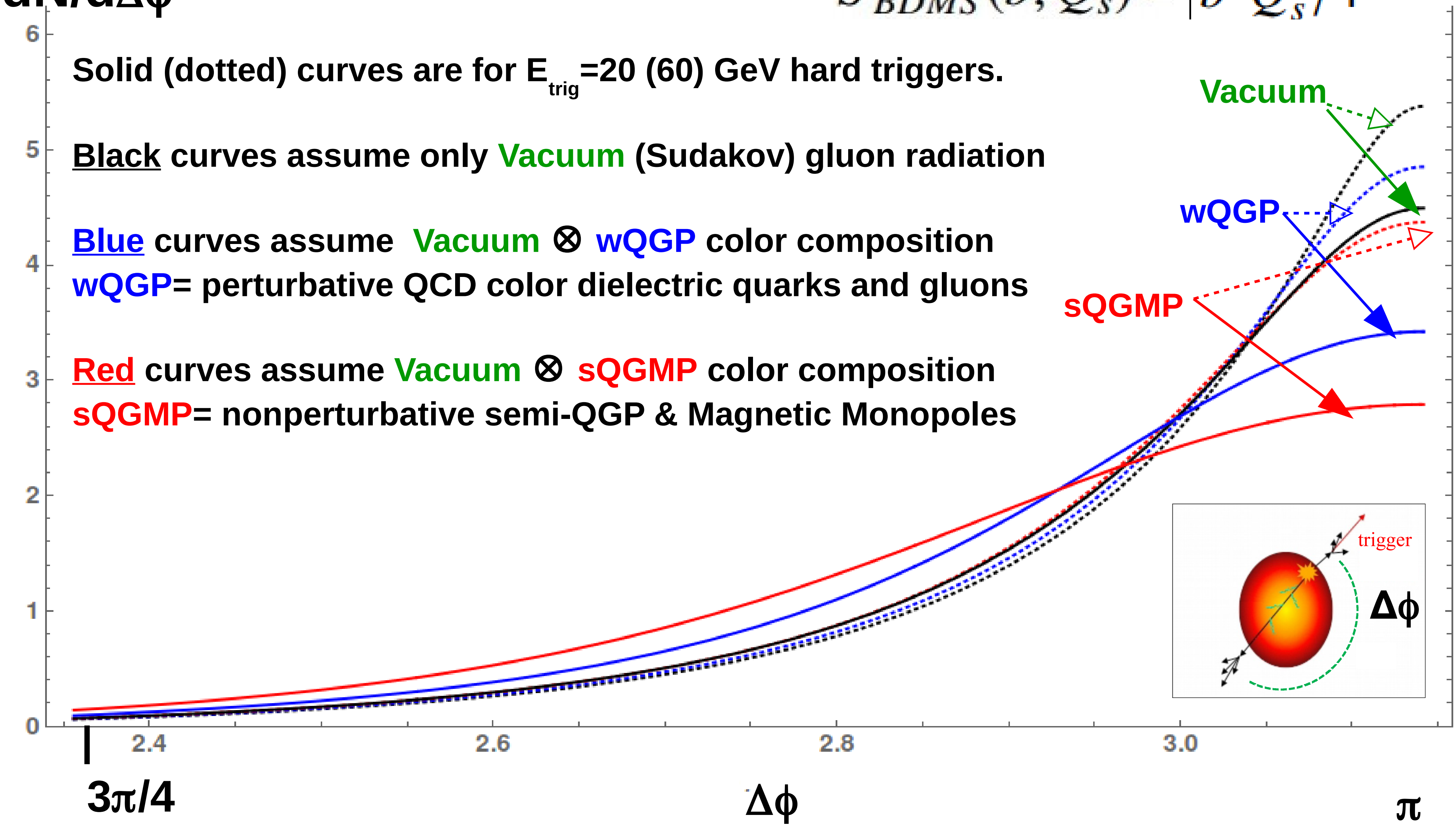

Caveat: Unfortunately a fit to the intercept at $\Delta\phi=\pi$ does not uniquely define Q_s^2

Need also shape analysis $\Delta\phi$ to distinguish between Gaussian and Yukawa forms:

The medium induced broadening in **one parameter** multi soft **Gaussian** BDMS approximation

BDMS (Gaussian) dipole approx:

$$S_{BDMS}(b;Q_s) = b^2 Q_s^2/4$$

$$Q_s^2 = \int dt\ \hat{q}(T(\vec{r}(t),t)),Q)$$

The **two parameter** (opacity **χ=L/λ** and screening **μ**) GLV multiple Yukawa scatt approx:

$$S_{GLV}(b;\chi,\mu) = \chi(\mu b K_1(\mu b) - 1) \approx b^2 \underline{\log[1/(b\mu)^2]}(\chi\mu^2)/4$$

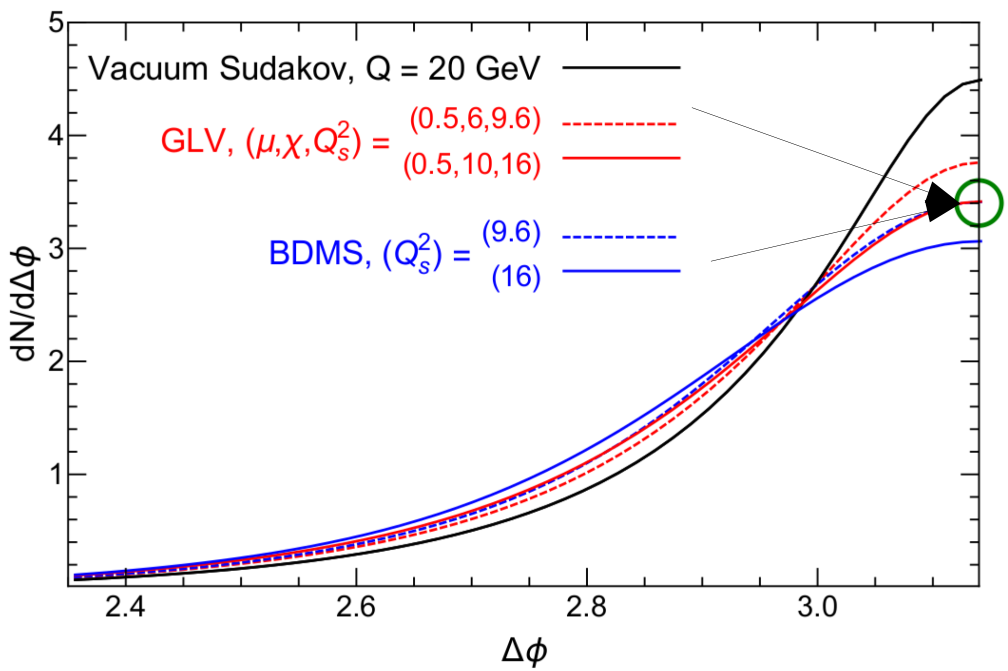

$$R(\Delta\phi;\chi,\mu) = dN_{AA}/dN_{pp}$$

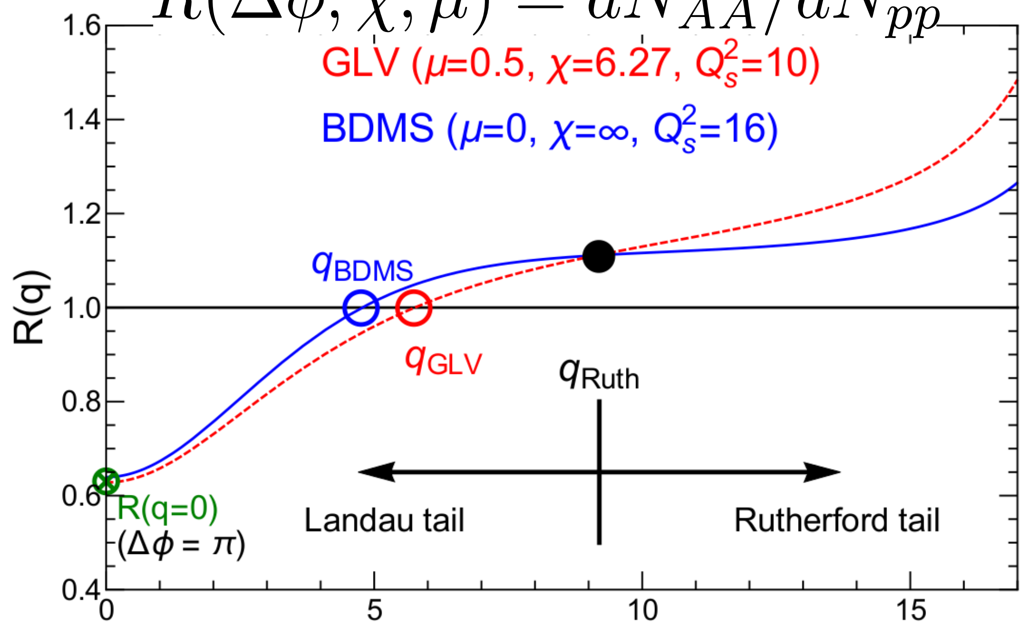

$$q = E_{trig}\Delta\phi$$

Need Pecent level precision on acopl shape to resolve Rutherford tails

Section 2: Open Problems

Radiative Corrections to elastic scattering

Elastic Straggling of a heavy b quark and acoplanarity

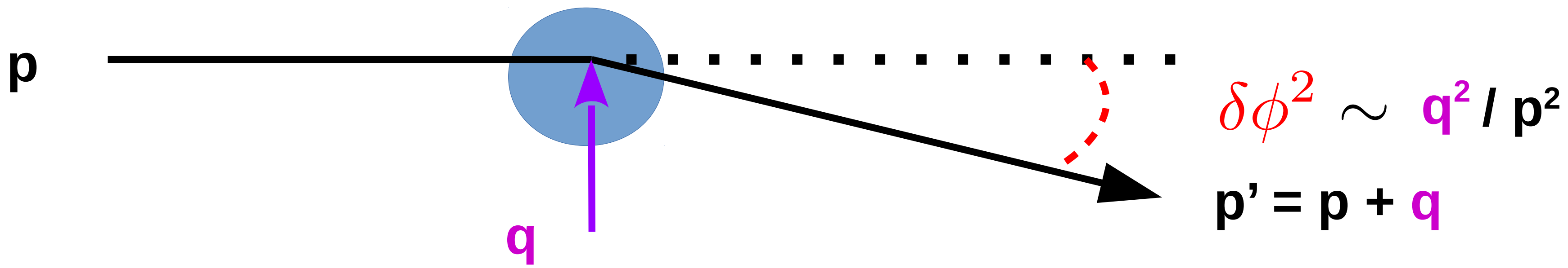

Radiative g Correction to Elastic Straggling of a heavy b quark and acoplanarity correction

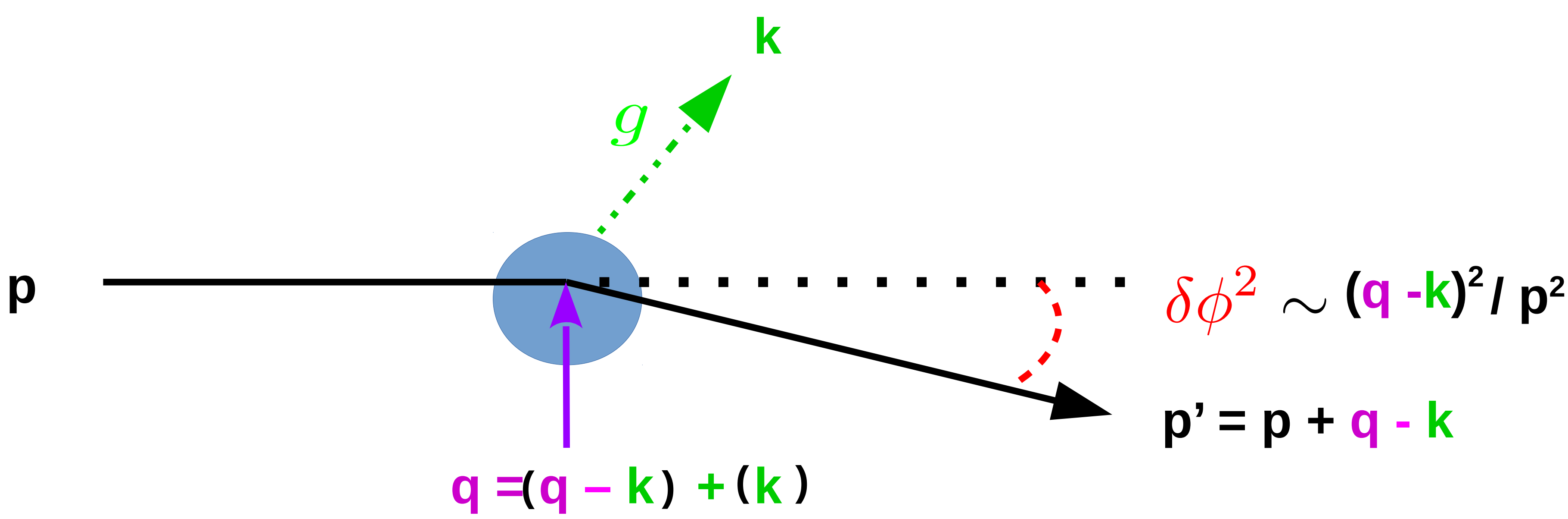

30 T. Liou, A. H. Mueller, and B. Wu, Nucl. Phys. **A916**, 102 (2013), 1304.7677.
31 J.-P. Blaizot and Y. Mehtar-Tani, Nucl. Phys. **A929**, 202 (2014), 1403.2323.
32 J.-P. Blaizot and F. Dominguez, Phys. Rev. **D99**, 054005 (2019), 1901.01448.
33 E. Iancu, P. Taels, and B. Wu, Phys. Lett. **B786**, 288 (2018), 1806.07177.

Static brick
Length L

$$\boxed{\hat{q}_{rad}(L) \approx \hat{q}_{el} \frac{\bar{\alpha}}{2} \log^2(L/\ell_0)\,,} \quad \begin{array}{l} \sim 0.4\ \hat{q}_{el} \text{ For L~5 fm} \\ \sim 0.2\ \hat{q}_{el} \text{ For L~3 fm} \end{array}$$

d-dim expansion $\hat{q}(t) = \hat{q}(t_0)(t_0/t)^{d/3}$

$$\boxed{\hat{q}_{rad}(L, t_0, d) = \hat{q}_{el} \frac{\bar{\alpha}}{2} (1 - d/3)^2 \log^2(L/\ell_0)\,.}$$

$$\int_{\hat{q}\tau_{\min}}^{\hat{q}L} \frac{d\boldsymbol{k}^2}{\boldsymbol{k}^2} \int_{k^2\tau_{\min}}^{k^4/\hat{q}} \frac{d\omega}{\omega} + \int_{\hat{q}L}^{\boldsymbol{p}^2} \frac{d\boldsymbol{k}^2}{\boldsymbol{k}^2} \int_{k^2\tau_{\min}}^{k^2 L} \frac{d\omega}{\omega}$$

$$\hat{q}_{rad}/\hat{q}_{el} \sim \alpha_s \left[= \frac{1}{2} \ln^2 \frac{L}{\tau_{\min}} + \ln \frac{L}{\tau_{\min}} \ln \frac{\boldsymbol{p}^2}{\hat{q}L}. \right] \sim 1$$

Does radiative correction Double elastic aoplanarity ??

Radiative contribution to $p_\perp$-broadening of fast partons in a quark-gluon plasma

B.G. Zakharov[1]

[1]L.D. Landau Institute for Theoretical Physics, GSP-1, 117940, Kosygina Str. 2, 117334 Moscow, Russia

(Dated: December 11, 2019)

The contribution of radiative processes to $p_\perp$-broadening of fast partons in a quark-gluon plasma is investigated. Calculations are performed beyond the soft gluon approximation. It is shown that the radiative correction to $\langle p_\perp^2 \rangle$ for conditions of heavy ion collisions at RHIC and LHC is negative and can be comparable in absolute value with the nonradiative contribution. This prediction differs radically from the essentially positive contribution of radiative processes to $p_\perp$-broadening, which was predicted earlier in the literature.

The total contribution to $\langle p_\perp^2 \rangle_{rad}$ corresponding to the sum $F + \tilde{F}$ can be written as the sum of three terms

$$\langle p_\perp^2 \rangle_{rad} = I_1 + I_2 + I_3 \,, \tag{88}$$

Using the values of the ratio $\hat{q}'/\hat{q}$ from (96), we obtain from relations (97) and (98) the following values for the ratios of the radiative and nonradiative contributions in our versions for RHIC(LHC)

$$\langle p_\perp^2 \rangle_{rad}/\langle p_\perp^2 \rangle_0 \approx -0.598(-0.629)\,,\ r = 1.94(2.13)\,. \tag{99}$$

And for $\hat{q}' = \hat{q}$ we obtain

$$\langle p_\perp^2 \rangle_{rad}/\langle p_\perp^2 \rangle_0 \approx -0.397(-0.192)\,,\ r = 1(1)\,. \tag{100}$$

It can be seen that even in the version disregarding the difference between $\hat{q}'$ and $\hat{q}$, the radiative contribution to the $p_\perp$-broadening turns out to be negative for the RHIC and LHC conditions.

In CUJET3 the radiative correction to elastic energy loss is

For our application here, note that $\tilde{\boldsymbol{q}}_\perp \equiv \boldsymbol{q}_\perp - \boldsymbol{k}_\perp$ is the actual jet recoil associated with radiating a gluon with transverse momentum $\boldsymbol{k}_\perp$. In order to compute the radiative correction to the elastic $\hat{q}_{el}$ we must then perform the integration over $\int d^2\boldsymbol{q} d^2\boldsymbol{k} \cdots$ weighed with an extra factor of $(\boldsymbol{k}_\perp - \boldsymbol{q}_\perp)^2 = \Omega^2 - m^2$. However, since $\Delta\hat{q}_{rad} = \langle \tilde{\boldsymbol{q}}_\perp^2 / \lambda \rangle$ we must also remove the factor of x in the curly brackets of the ΔE_{rad} functional Eq.3. Thus, the radiative correction, $\Delta Q^2_{rad} = \langle N_g \rangle \langle (\boldsymbol{q} - \boldsymbol{k})^2$ to the elastic saturation scale squared can be calculated in CUJET3 using

$$\begin{aligned} \Delta Q^2_{rad}[a, \vec{z}(t)] &\equiv \int dN_g(t) \, \{(\boldsymbol{q}-\boldsymbol{k})^2\} = \int dt d^2\boldsymbol{q} \int dx d^2\boldsymbol{k} \, \frac{dN_g(t)}{dt d^2\boldsymbol{q} dx d^2\boldsymbol{k}} \, \{(\boldsymbol{q}-\boldsymbol{k})^2\} \\ &= C_a \int dt d^2\boldsymbol{q} \, \Gamma_g(\boldsymbol{q}, t) \int \frac{dx}{x} d^2\boldsymbol{k} \, \bar{\alpha} \, A(\boldsymbol{k}, \boldsymbol{q}, t) \, P(t | x E_0, \boldsymbol{k}, \boldsymbol{q}) \, \{(\boldsymbol{q}-\boldsymbol{k})^2\} \, , \end{aligned} \tag{10}$$

Turns out to be negative due to near field interference between N=0 and N=1 amplitudes
In qualitative agreement with Zakharov claim.

$$\Delta Q^2_{rad} / \Delta Q^2_{elas} \sim -0.5 \;!!$$

In both sQGMP and wQGP dof

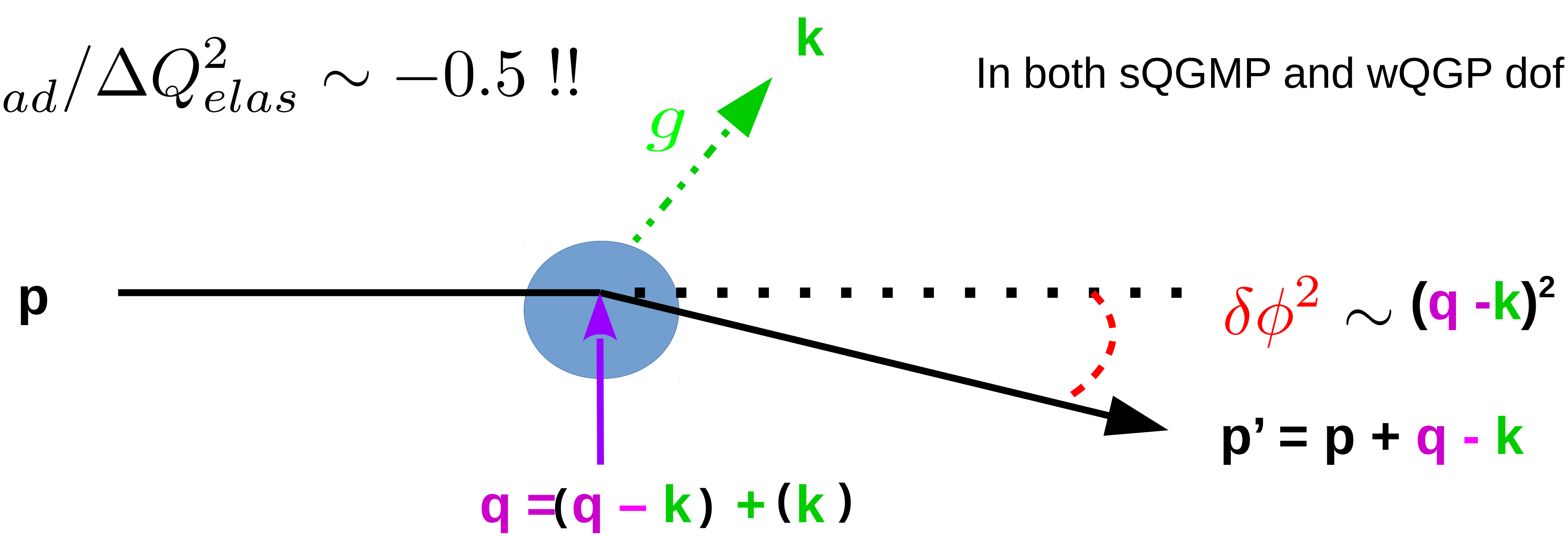

The total elastic recoil q is SHARED between emitted gluons and the leading parton

Section 3:   Concluding Remarks

ALICE et al, JHEP 09 (2015) 170

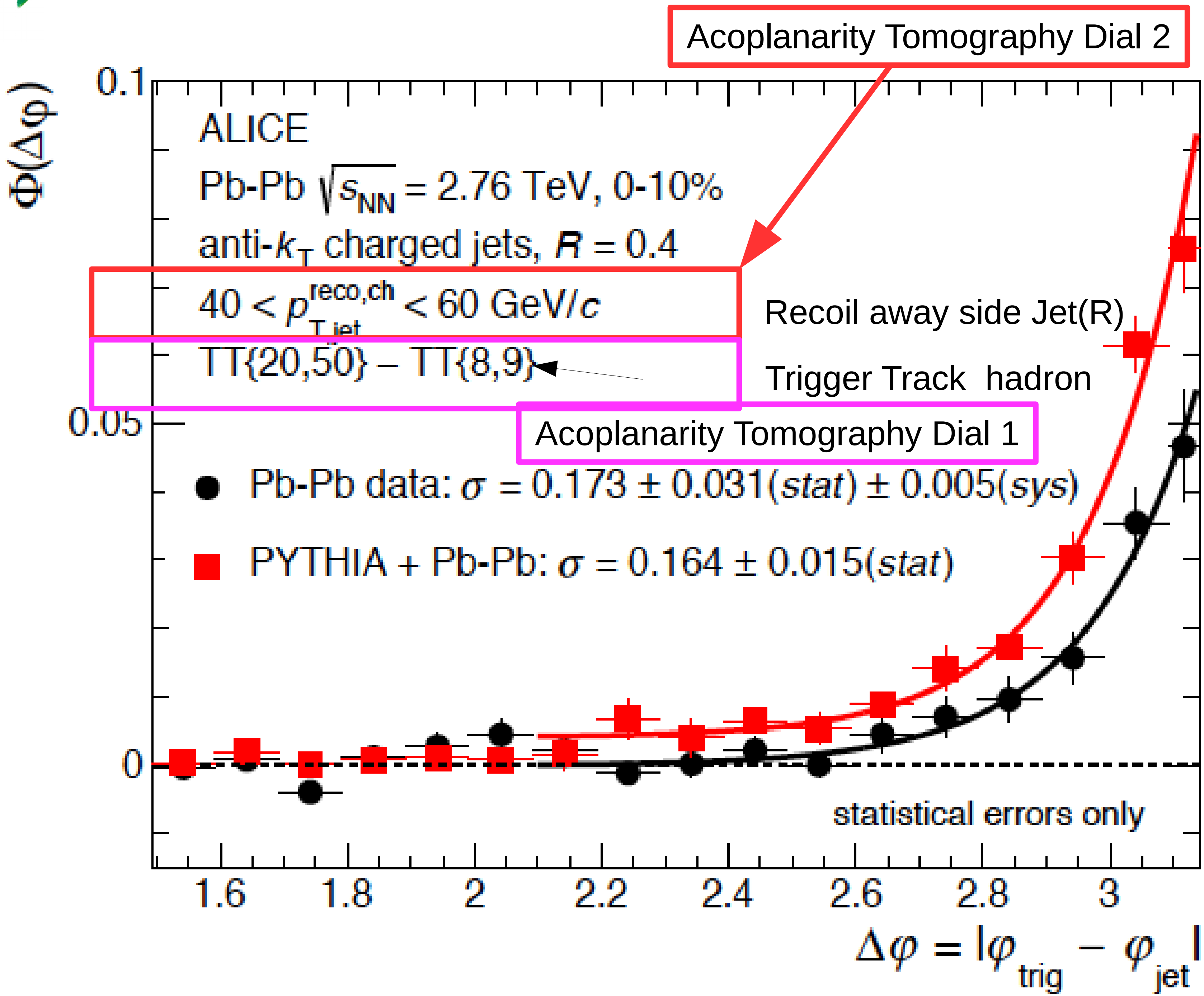

Single Jet trigger surface bias depends on jet Casimir q=4/3 or g=3

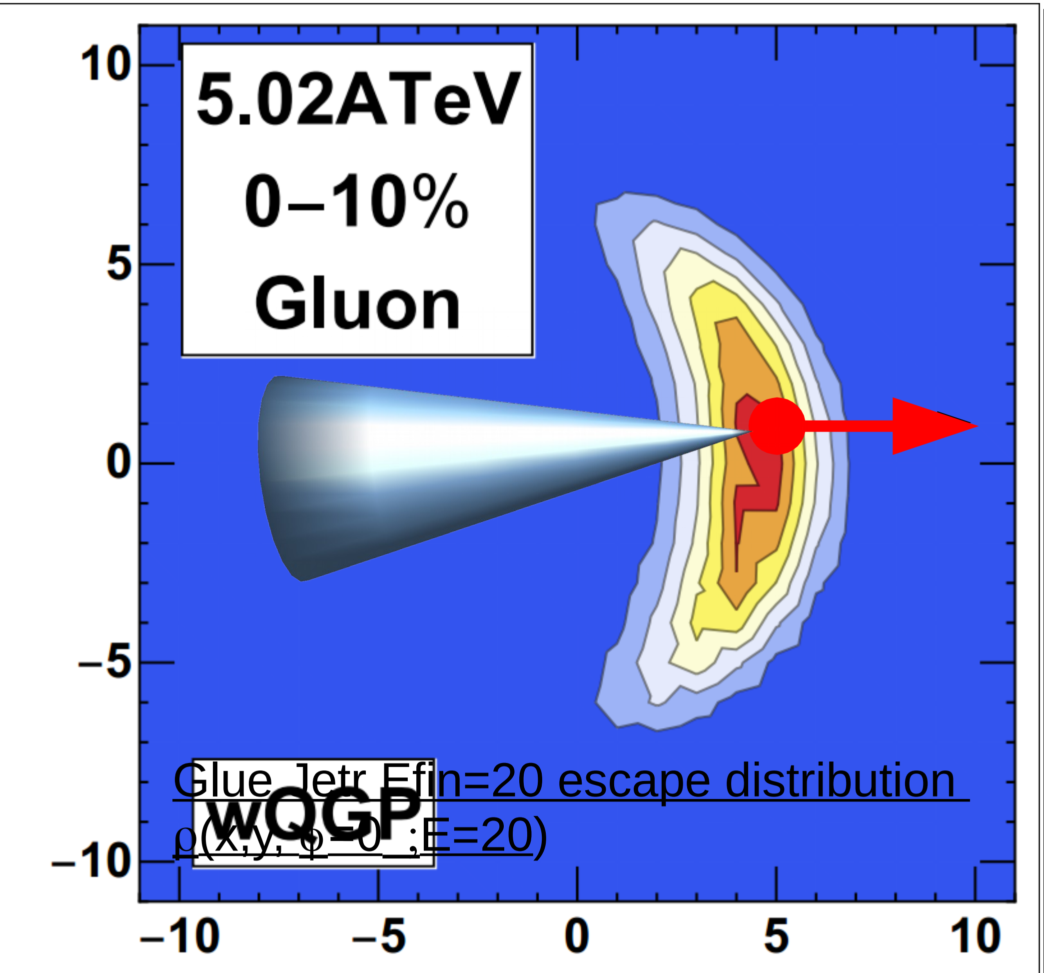

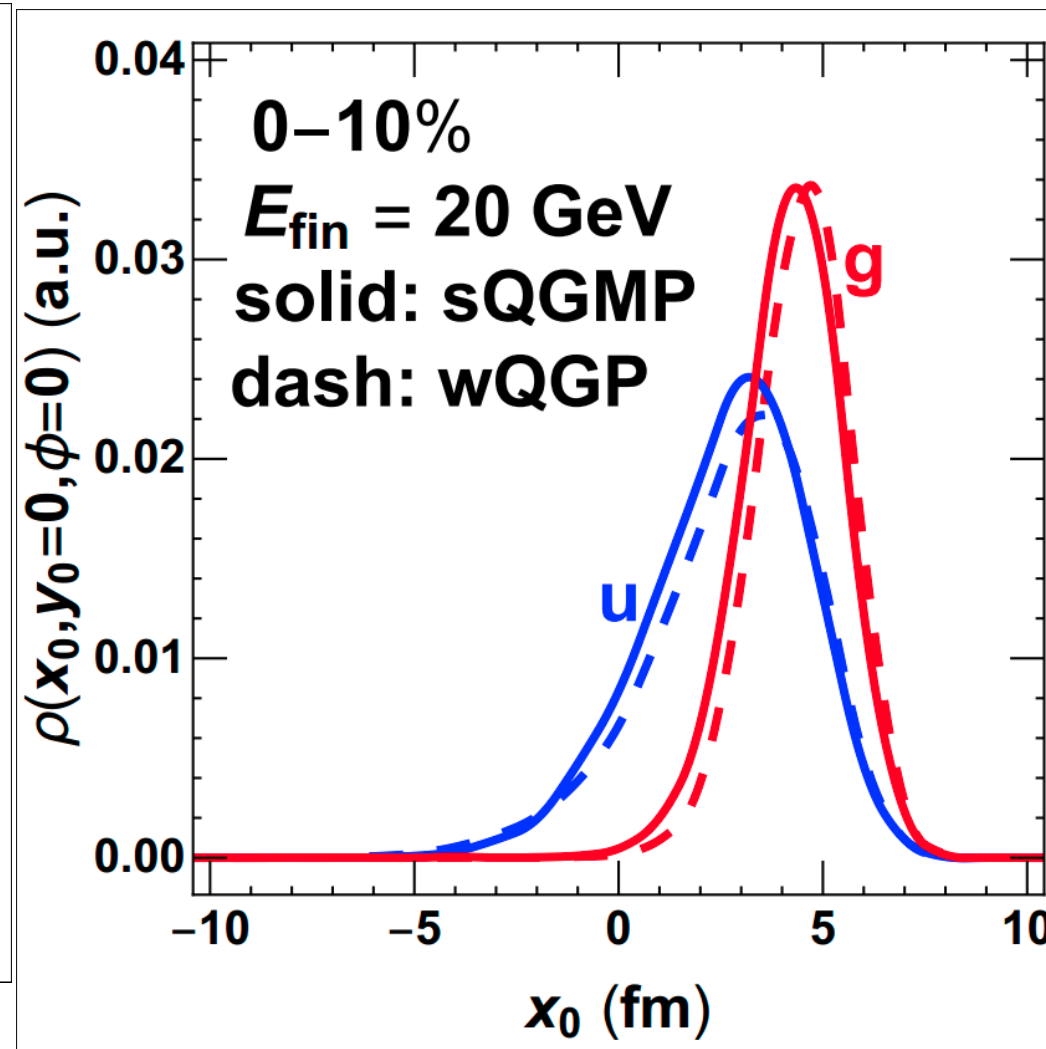

However, CUJET shows that the bias is ***independent*** of the color composition of fluid

IF coupling is constrained by global Chi^2 fit to RHIC+LHC data on **RAA**(pT; s, cent%)

Implies that Jet Acoplanarity is mostly sensitive to T(x,t) ~ (1-2)Tc hypersurface

MGyulassy **Acoplanarity is more sensitive to possible Non-perturbative Opalescence near Tc**

The Medium induced Acoplanarity *correction* to vacuum Sudakov requires consistent calculation of dijet energy loss as well as dijet azimuthal straggling transverse to initial dijet axis

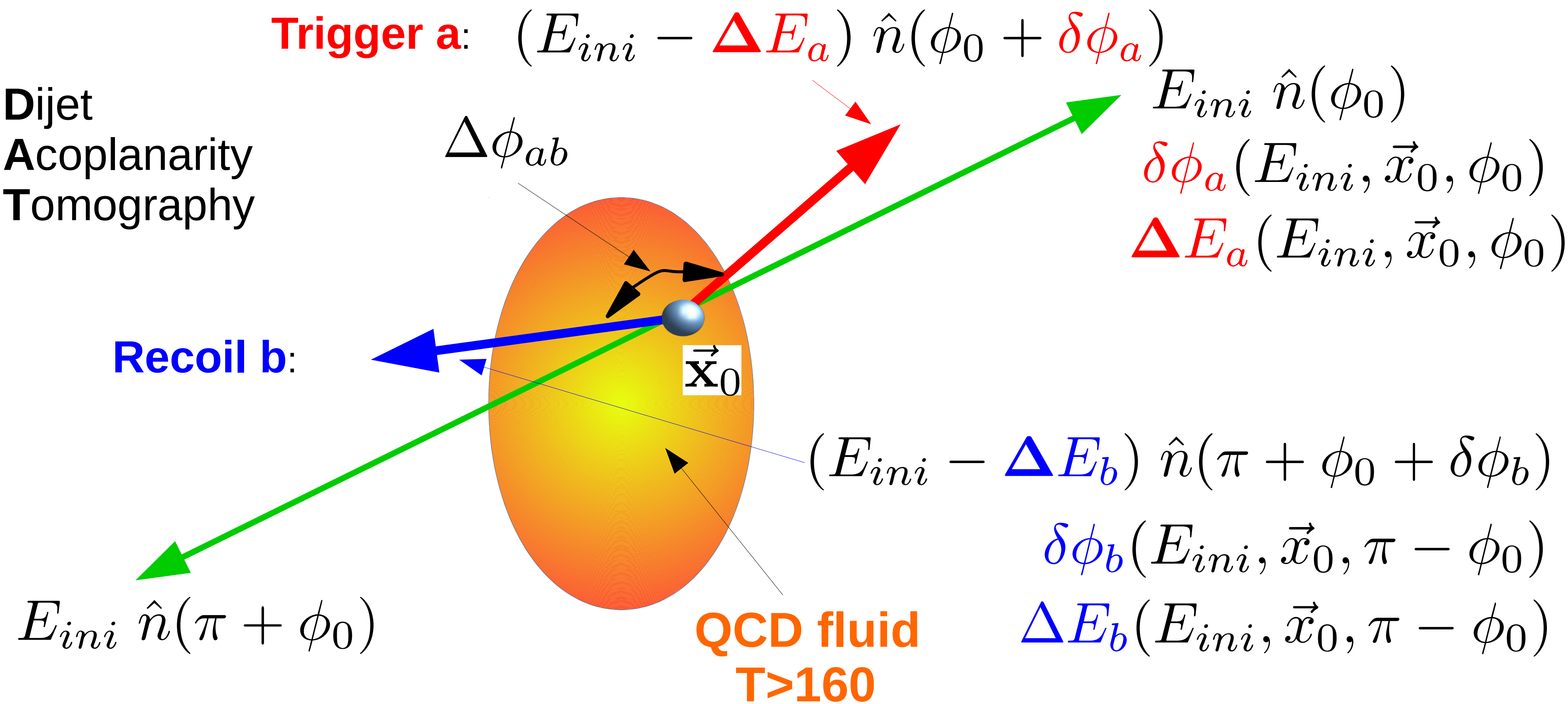

Azimuthal Acoplanarity Width^2

$$\Delta\phi^2_{ab} = \Delta\phi^2_{ab}[vac] + \Delta\phi^2_{ab}[med]$$

$$\approx \mathbf{C}\alpha_s + \left(\mathbf{Q}^2_a[\phi_0, \vec{x}_0] + \mathbf{Q}^2_b[\pi + \phi_0, \vec{x}_0]\right) / E^2_{ini}$$

Dijet partons **a**+**b** → h^{ch}(trigger) + Away side reconstructed jet

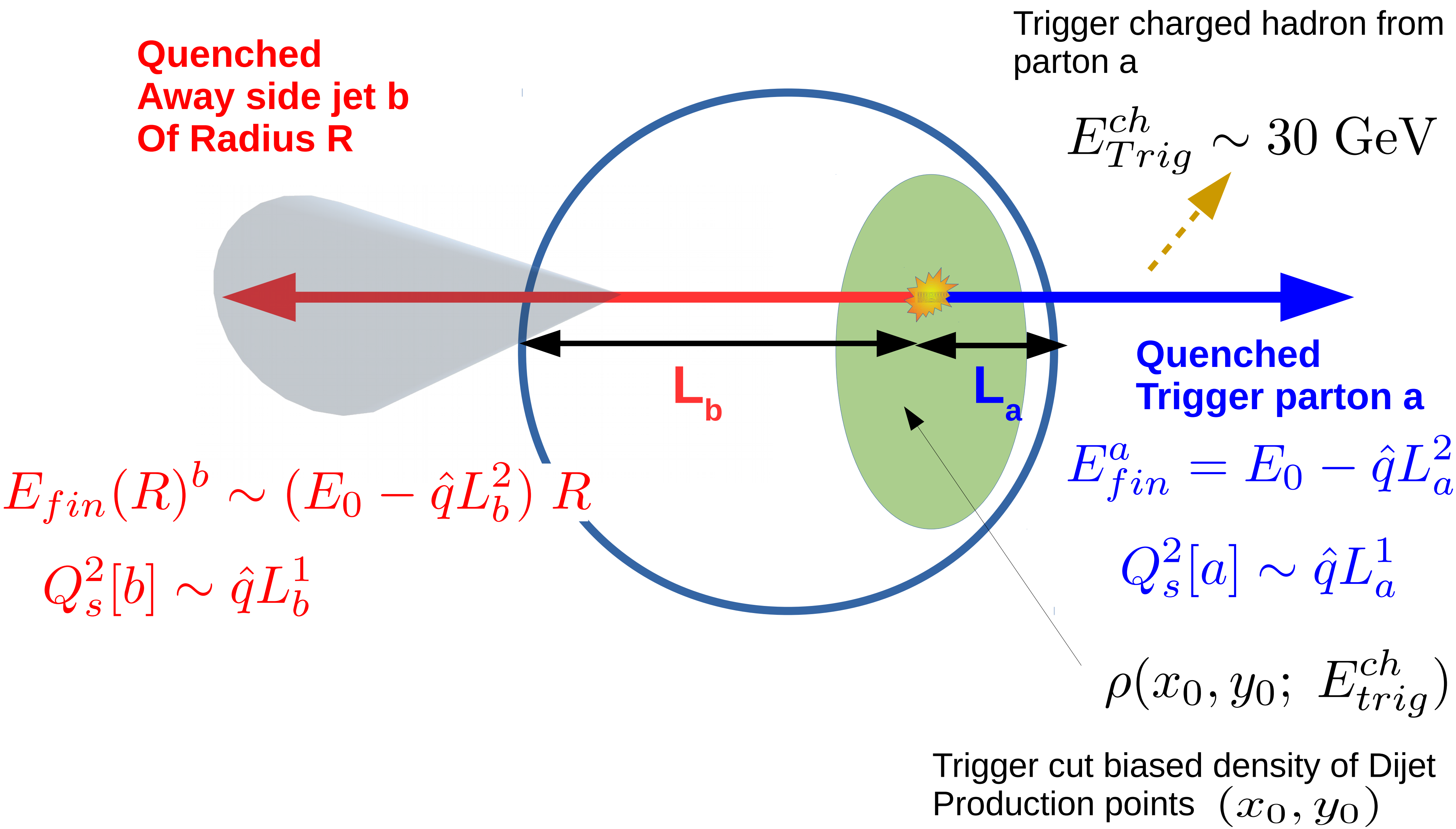

Could ALICE *current* $40 < E_{T,jet}^{recon,ch} < 60$ GeV high jet cut bias acoplanarity away ??

Dijet partons **a**+**b** → h^{ch}(trigger) + Away side reconstructed jet

Hadron-Jet energy cuts
biased density

$$\rho_{ab}(x_0, y_0;\ E_{trig}^{ch},\ E_{jet}(R))$$

Trigger charged hadron from
parton a

Quenched
Away side jet b
Of Radius R

$$E_{Trig}^{ch} \sim 30 \text{ GeV}$$

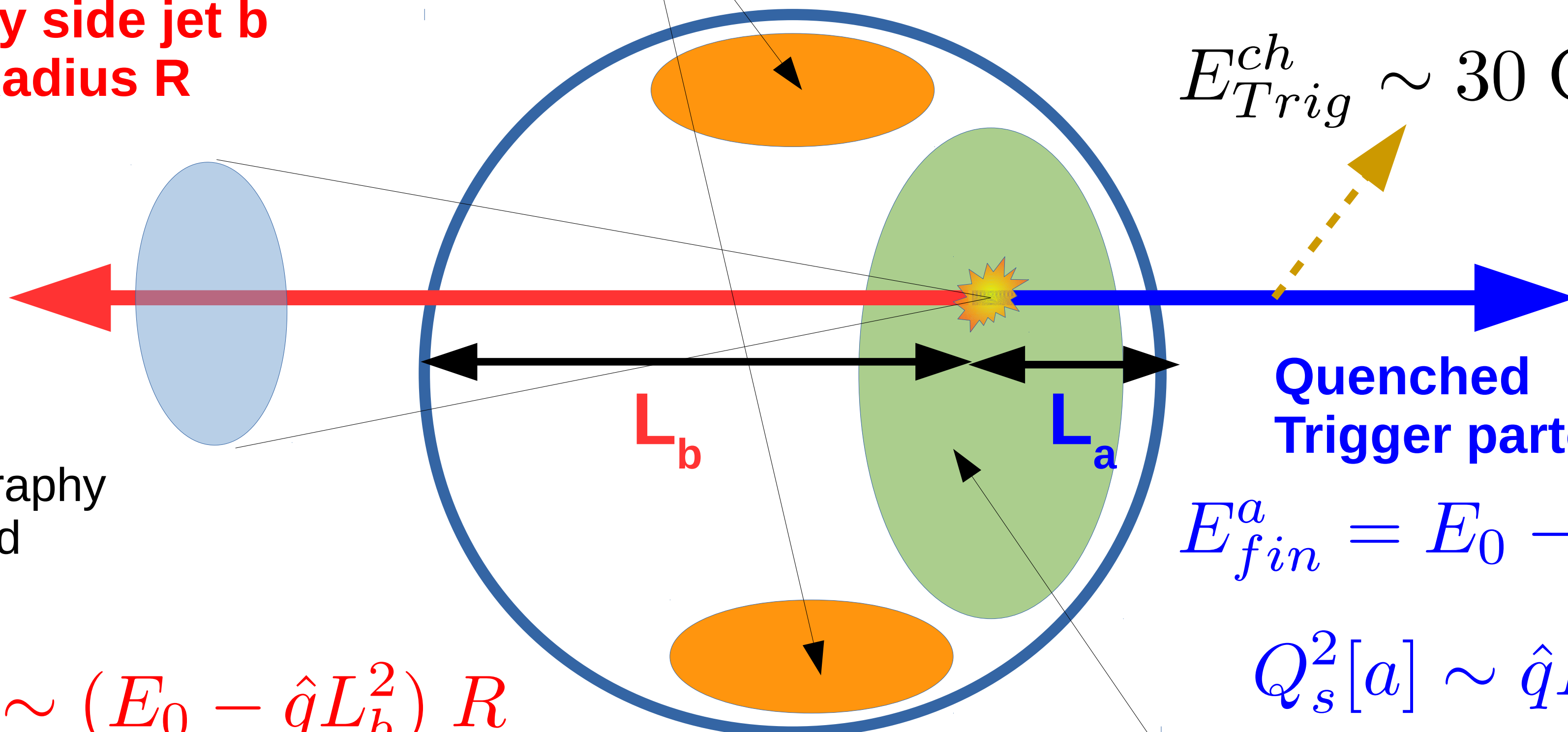

Quenched
Trigger parton a

$$E_{fin}^{a} = E_0 - \hat{q}L_a^2$$

$$Q_s^2[a] \sim \hat{q}L_a^1$$

2D Tomogbraphy
of QCD Fluid

$$E_{jet}^{b}(R) \sim (E_0 - \hat{q}L_b^2)\ R$$

$$Q_s^2[b] \sim \hat{q}L_b^1$$

$$\rho_a(x_0, y_0;\ E_{trig}^{ch})$$

A too high min jet cut may strongly distort quenched geom

$$E_{jet}^{b}(R) > E_{min} = 40$$

Trigger cut biased density of Dijet
Production points (x_0, y_0)

Summary :

R_{AA} & v_n ***Constrained*** Dijet Acoplanarity Tomography can help to falsify competing models of the color d.o.f. in perfect QCD fluids produced at RHIC and LHC

Hard Trigger

(Q, ϕ_1)

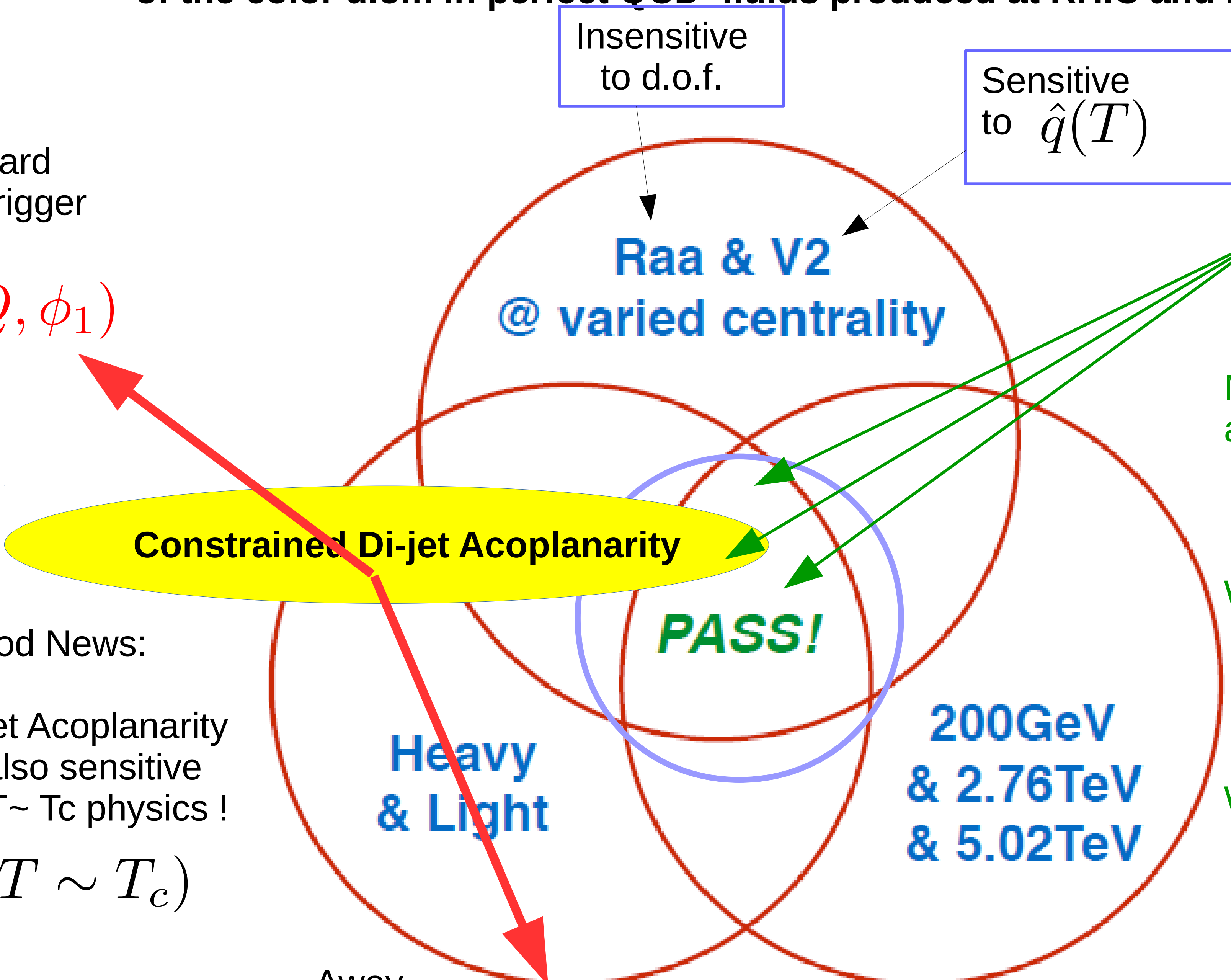

Good News:

Dijet Acoplanarity is also sensitive to T~ Tc physics !

$$\hat{q}(T \sim T_c)$$

Multiple models are consistent with current data RHIC&LHC

We still do not know what are color dof of QCD perfect fluids!

We need other independent observables that probe dof

Away Side Jet

ϕ_2

Bottom Line: Future percent level precision will be needed experimentally on $dN/d\Delta\phi$